CARBON DIOXIDE REDUCTION IN REVERSE FLOW REACTORS

A THESIS SUBMITTED TO
THE GRADUATE SCHOOL OF NATURAL AND APPLIED SCIENCES
OF
MIDDLE EAST TECHNICAL UNIVERSITY

BY
NEVZAT CAN AKSU

IN PARTIAL FULFILLMENT OF THE REQUIREMENTS
FOR
THE DEGREE OF MASTER OF SCIENCE
IN
CHEMICAL ENGINEERING

DECEMBER 2013

Approval of the thesis:

CO$_2$ REDUCTION IN REVERSE FLOW REACTORS

submitted by **NEVZAT CAN AKSU** in partial fulfillment of the requirements for the degree of **Master of Science in Chemical Engineering Department, Middle East Technical University** by,

Prof. Dr. Canan Özgen   _____
Dean, Graduate School of **Natural and Applied Sciences**

Prof. Dr. Deniz Üner   _____
Head of Department, **Chemical Engineering**

Prof. Dr. Deniz Üner   _____
Supervisor, **Chemical Engineering Dept., METU**

Engineer. M. Sc. İbrahim Bülent Atamer   _____
Co-supervisor, **Terralab**

Examining Committee Members:

Prof. Dr. Halil Kalıpçılar   _____
Chemical Engineering Dept., METU

Prof. Dr. Deniz Üner   _____
Chemical Engineering Dept., METU

Assoc. Prof. Nuray Oktar   _____
Chemical Engineering Dept., Gazi University

Dr.Harun Koku   _____
Chemical Engineering Dept., METU

Engineer. M. Sc. İbrahim Bülent Atamer   _____
Terralab

                     Date: _____

I hereby declare that all information in this document has been obtained and presented in accordance with academic rules and ethical conduct. I also declare that, as required by these rules and conduct, I have fully cited and referenced all material and results that are not original to this work.

Name, Last name: Nevzat Can Aksu

Signature:

ABSTRACT

CO$_2$ REDUCTION IN REVERSE FLOW REACTORS

Aksu, Nevzat Can
M. Sc. Department of Chemical Engineering
Supervisor: Prof. Dr. Deniz Üner
Co supervisor: İbrahim Bülent Atamer

December 2013, 76 pages

Syngas, a mixture of CO and H$_2$, is a very important industrial gas mixture, because it can be used for synthesizing products such as synthetic natural gas, ammonia and methanol. The main purpose of this work was to obtain CO by CO$_2$ reduction. Reducible metal oxides are used as catalysts due to the fact that they can be reduced and re-oxidized upon changes in temperature, pressure and gas atmosphere. CeO$_2$ was chosen for this cyclic reaction pathway based on the reports on similar studies in literature. It is preferred due to its not toxic nature and it high melting point. Pt was used to lower the oxygen desorption temperature and Al$_2$O$_3$ was also used to get higher surface area.

Reversed flow reactors (RFR) work by changing the gas flow direction periodically as its name indicates. This type of reactor is used in various applications in industry. Oxidation-Reduction reactions are also very suitable for this reactor because materialin the reactor can be used as a heat sink for one exothermic and one endothermic reaction.

In order to study the red-ox properties of the selected material, TPD analyses of Al$_2$O$_3$, Al$_2$O$_3$-CeO$_2$, Pt/CeO$_2$ and Pt/Al$_2$O$_3$-CeO$_2$ were performed. Two different methods were used to prepare the samples. These are the incipient wetness method and the polyol method. Effects of sample preparation methods and Pt amount in sample were investigated. H$_2$O and CO$_2$ adsorption/desorption amounts for the samples that have different loadings of Pt were investigated. It was shown that H$_2$O and CO$_2$ adsorption/desorption amount increases with increasing Pt concentration in the catalyst. The H$_2$O adsorption amount of the catalyst that has 1% Pt is 1.58 times the amount of catalysis that has 0.5% Pt. CO$_2$ adsorption amount of catalysis that has 1% Pt is about 4.5 times the amount of catalysis that has 0.5% Pt.

Desorption orders of H_2O and CO_2 from Pt/Al_2O_3-CeO_2 were found to be first order and second order respectively. Thermodynamic analysis of equilibrium conversion of the red-ox reaction supports that CeO_2 is turned to Ce_2O_3 after oxygen desorption. The results of thermodynamic calculations show that there is no oxygen desorption up to 1400 ^{0}C. This situation is also demonstrated by TPD experiments. When 1% Pt was added to the surface of CeO_2, oxygen desorption peak was observed at about 900 ^{0}C. These experiments indicate that Pt can lower oxygen desorption temperature.

One of the purposes of this thesis was to construct an automated flow reversal temperature programmed desorption system and making and analyzing TPD experiments. An automatic flow reversal system was designed and constructed to make cyclic reduction and oxidation reactions with metal oxides. The system was also tested in this work and it is seen that the system can work properly. During these tests, the effect of high surface area that was obtained by using Al_2O_3 on oxygen desorption is demonstrated.

In addition to all of these, oxygen desorption experiments were made by the catalysts that were prepared by two different methods. Experiments show that the catalyst which was prepared by polyol method has 10 times more oxygen desorption amount than the catalyst which was made by incipient wetness method. By this way, effect of Pt dispersion on the oxygen evolution from the catalyst surface was demonstrated.

ÖZ

TERS AKIŞLI REAKTÖRLERDE CO_2 İNDİRGENMESİ

Aksu, Nevzat Can
Yüksek Lisans, Kimya Mühendisliği Bölümü
Tez Yöneticisi: Prof. Dr. Deniz Üner
Ortak Tez Yöeticisi: İbrahim Bülent Atamer

Aralik 2013, 76 sayfa

CO ve H_2 karışımından oluşan sentez gazı endüstriyel değeri olan önemli bir gaz karışımdır. Bunun sebebi sentetik doğal gaz, amonyak ve metanol gibi ürünlerin bu gaz karışımından sentezlenebilmesidir. Bu çalışmanın temel amacı CO_2 gazının indirgenmesi ile CO gazını elde edebilmektir. Metal oksitler, sıcak, basınç ve ortamdaki gaz kompozisyonundaki değişikliklere göre indirgenebildikleri ve yükseltgenebildikleri için bu amaç için kullanabilmektedirler. Literatürde bulunan benzer çalışmalara dayanılarak bu döngüsel reaksiyon serisinde kullanılmak üzere seçilmiştir. CeO_2, zehirli olmaması ve erime noktasının yüksek olması nedeniyle tercih edilmiştir. Oksijen desorpsiyon sıcaklığının aşağı çekilebilmesi amacıyla Pt ve yüzey alanını artırmak amacıyla da Al_2O_3 kullanılmıştır.

Ters akışlı reaktörler isminden anlaşılabileceği gibi gaz akış yönlerinin periyodik bir şekilde değişmesi prensibiyle çalışırlar. Bu tip reaktörler endüstride çeşitli amaçlarla kullanılırlar. Oksidasyon-redüksiyon reaksiyonları bu tip reaktörler için oldukça uygundur çünkü bir ekzotermik biri endotermik olan reaksiyon çiftlerinde, reaktörün içerisindeki materyal ısı emici görevi görebilir.

Al_2O_3, Al_2O_3-CeO_2, Pt/CeO_2 ve Pt/Al_2O_3-CeO_2'nın redoks özelliklerinin belirlenebilmesi için SPD analizleri yapılmıştır. Örneklerin hazırlanması için iki ayrı metod kullanılmıştır. Bu metodlar ıslaklık başlangıcı emdirme metodu ve polyol metodudur. Sentez metodların ve malzemedeki Pt miktarının etkileri incelenmiştir. H_2O ve CO_2 adsorpsiyon ve desorpsiyon miktarlarının katalizördeki Pt miktarına baplı olarak arttığı gösterilmiştir. % 1 Pt içeren katalizörün H_2O adsorplama miktarının % 0.5 Pt içerenden 1.58 kat fazla, CO_2 adsorplama miktarının ise yaklaşık 4.5 kat fazla olduğu belirlenmiştir. H_2O ve CO_2 moleküllerinin

Pt/Al$_2$O$_3$-CeO$_2$ kazalizöründen desorplanma mertebesi H$_2$O için birinci mertebe olarak CO$_2$ için ise ikinci mertebe olarak hesaplanmıştır. Oksijen desorplamasıyla CeO$_2$'in Ce$_2$O$_3$'e dönüşebildiği redoks reaksiyonun denge dönüşüm oranının termodinamik analizi ile desteklenmiştir. Analiz sonuçları, oksijen desorpsiyonun 1400°C'ye kadar gerçekleşmeyeceğini göstermiştir. Bu durum ayrıca SPD deneyleri ile de desteklenmiştir. CeO$_2$'in yüzeyine 1%Pt yüklendiği zaman oksijen desorpsiyon'un 900°C civarlarında bır maksımum verdiği gözlemlenmiştir. Bu deneyler Pt'in oksijen desorpsiyon sıcaklığını düşürebildiğini göstermiştir.

Bu tezin amaçlarının biri de otomatik ters akışlı sıcaklık programlı desorpsiyon sistemi yapmak ve SPD deneylerini bu sistem üzerinde gerçekleştirebilmektir. Otomatik ters akışlı sıcaklık programlı desorpsiyon sistemi tasarlandı ve metal oksitlerin döngüsel indirgenme ve yükseltgenme reaksiyonlarını gerçekleştirelebilmek için yapıldı. Bu sistem bu çalışmada test edildi ve sistemin başarılı bir şekilde çalıştığı gösterilmiştir. Bu testler sırasında, Al$_2$O$_3$'ün kullanılmasıyla elde edilen yüksek yüzey alanının oksijen desorpsiyonlanma üzerine etkisi ayrıca incelendi.

Bütün bunlara ek olarak, iki farklı sentez metoduyla hazırlanan katalizörler ile oksijen desorplanma deneyleri yapıldı. Polyol metoduyla sentezlenen katalizörün oksijen desorplanma miktarının ıslaklık başlangıcı emdirme metodu ile sentezlenen katalizöre göre 10 kat daha fazla oksijen salabildiği deneysel olarak gösterilmiştir. Bu yolla, Pt dağılımının kataizör yüzeyinden oksijen salınımına etkisi ayrıca gösterilmiştir.

Anahtar Kelimeler: SPD, Oksidasyon, İndirgeme, Al$_2$O$_3$, CeO$_2$, Pt, ters akışlı reaktör

ACKNOWLEDGEMENTS

TABLE OF CONTENTS

LIST OF TABLES

TABLES

LIST OF FIGURES

FIGURES

CHAPTER 1

INTRODUCTION

1.1 Forced Unsteady State Operations

Forced unsteady state operations (FUSO) is running processes with periodical variations of one or more parameter of the process. Forced unsteady state conditions (FUSC) rather than steady state ones have been studied since 1960s [1-4]. These unsteady state conditions can be;

- Temperature
- Composition
- Parameters to the inlet of process unit such as flow rate

The main problem is the selection of unsteady state conditions which can give promising advantages rather than steady state conditions. There can be two positive outlaws, when the FUSO process is performed in a heterogeneous catalytic reactor [5]:

1. Unsteady state conditions in the gas phase can give increase the changes in state, composition and structure of catalyst. This situation provides selectivity and /or activity increased according to steady state operations. This factor is called dynamic properties of the catalyst.

2. With variations of inlet parameters optimum temperature and composition distributions can be obtained which is not possible with steady state operations. This factor is called dynamic characteristics of a whole reactor system.

There are mainly three FUSO reactor types.

- Reversed Flow Reactors
- Loop Reactors
- Internal Recirculation Reactors

1.1.1 Reversed Flow Reactors

Reversed flow reactors (RFR) work by changing the gas flow direction periodically as its name indicates. Figure 1 illustrates the basic RFR configuration.
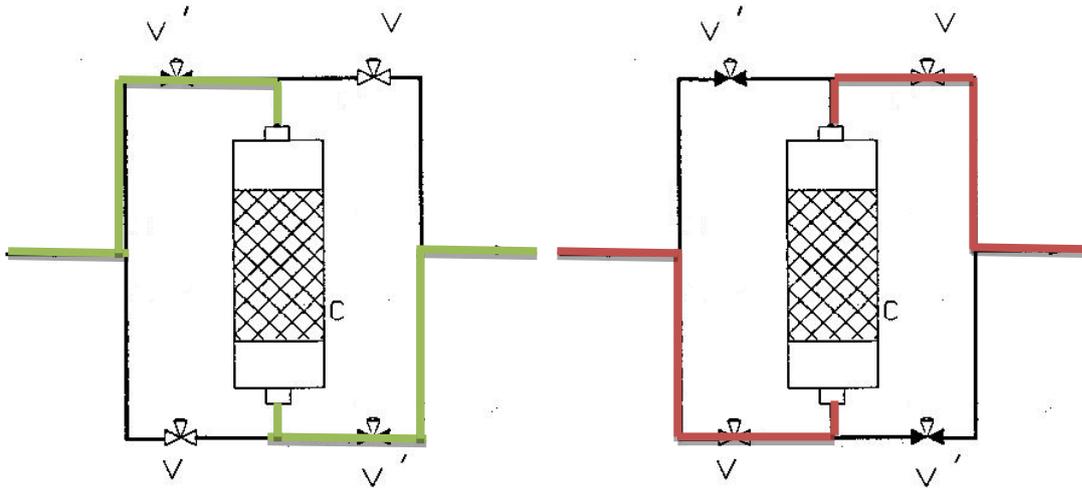
Figure 1. Reversed flow reactor diagram. V and V/ are switching valves

In the basic RFR configuration above, when $V^{/}$ valves are at open position, V valves are closed. After some time, V valves come to open position and at the same time $V^{/}$ valves getting close position. By this way, cyclic flow direction changes can be done.

RFR have some advantages for various types of reactions. The purpose of using RFR is that utilizing these advantages. There are four main advantages of RFR [5]:

1. Temperature Profile Regulation
2. Increasing Reaction Rate
3. Catalyst Deactivation/Regeneration
4. Cost Reduction

1.1.1.1 Advantages of RFR

1.1.1.1.1 Temperature Profile Regulation

Temperature profile regulation is a unique advantage for reversed flow operations (RFO) which for one route exothermic reaction, especially. SO_2 oxidation with vanadium oxide catalyst is a good example for that type RFO [6]. At the beginning, an inlet gas at $400^{0}C$ is fed into the system until the system reaches steady state. After that, an inlet gas at $200^{0}C$, at which SO_2 oxidation rate with vanadium oxide catalyst is negligible, is fed into the system from opposite direction. While the gas inlet side of the catalyst bed starts cooling slowly, the temperature at the center of the catalyst bed increases to higher temperatures than steady state temperature by this way. (Figure 2)
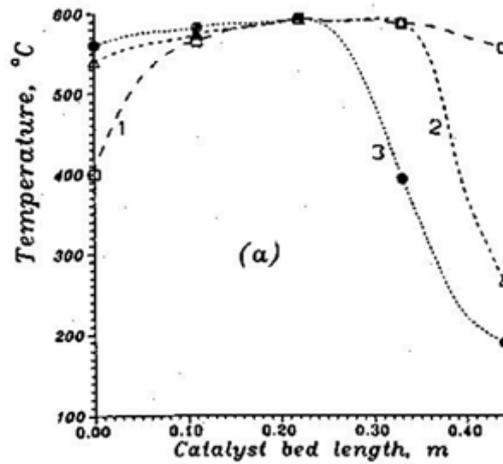
Figure 2. Temperature profile after first semi cycle in experimental reactor for SO_2 oxidation. 1, steady state for downward flow direction; 2, 60 min after cool gas feeding; 3, 120 min after cool gas feeding [6].

After 2 h, the flow direction of cool gas is changed. This time, the left part of the catalyst bed was started cooling while the right part of the bed was started heating. Temperature profiles after second cycle can be seen form Figure 3.

There is an important point that can be observed from the temperature diagram of reversed flow system. The difference between inlet temperature and maximum temperature in the reversed flow system is dramatically higher than the difference in the steady state system. It means that in the reversed flow system catalyst has two different functions. One of them is accelerating the chemical reaction and the other one is that the energy from the exothermic reaction is collected and transfered. This enables the use of the catalyst bed as heat exchanger for gas preheating.

3
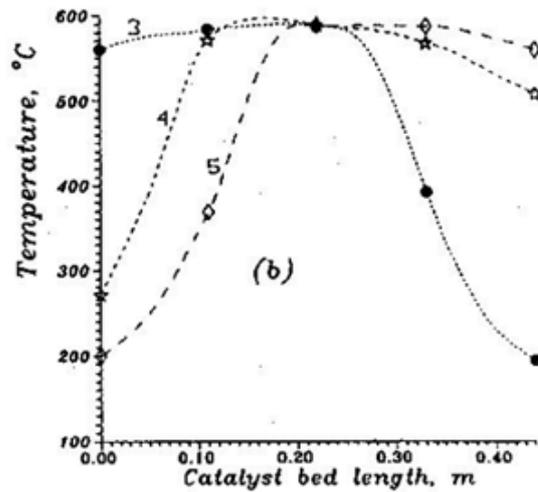
Figure 3. Temperature profile after second cycle in experimental reactor for SO_2 oxidation. 3, 60 min after first semi cycle; 4, 180 min after first flow changed; 3, 240 min after first flow changed [6].

1.1.1.1.2 Increasing Reaction Rate

One of the most important advantages of RFO is an increase in the reaction rate of a chemical reaction. The rise of reaction rate can be obtained by making an unsteady situation to temperature, concentration, residence time etc.

As it can be seen from Figure 3, temperature is decreased at the outlet of the reactor after the temperature plateau. It means the process conditions are near the equilibrium values. The reason of this observation is the large heat capacity of catalyst bed with respect to gas mixture. Conversion cannot be increased with increasing temperature for some reversible reactions which have thermodynamic limitations, such as SO_2 oxidation and ammonia synthesis. In industry, for these type of reactions, many catalytic stages with intermediate cooling are used. By employing RFO, higher conversion can be reached in a single catalyst bed than in a single catalyst bed for steady state operation [5, 6].

There is also another possible usage of RFO system by implementing very low frequency direction changes. By this way, a temperature oscillation can be observed in the system and this allows higher reaction rate values at same temperature than steady state system. CO oxidation reaction can be an example for such an advantage.In figure 6, conversion difference at the same temperature is shown. It can be easily seen by looking Figure 4, 5 and 6 [7].
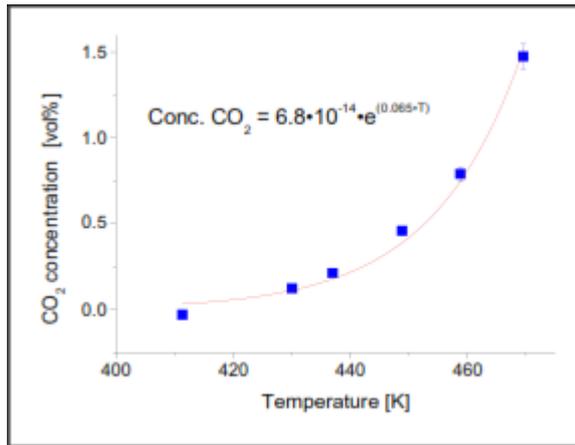
Figure 4. CO_2 concentration under stationary conditions by CO oxidation **[7]**
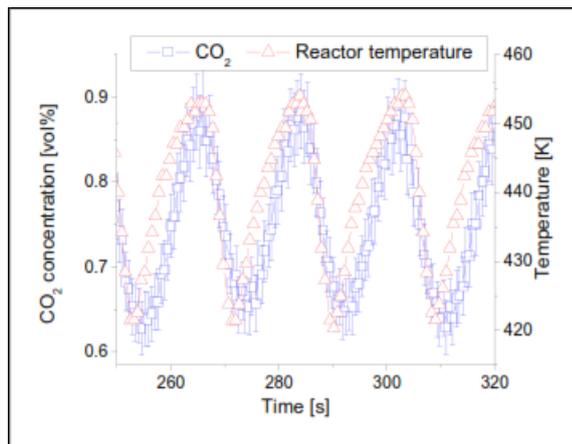
Figure 5. CO_2 concentration under forced system by CO oxidation **[7]**
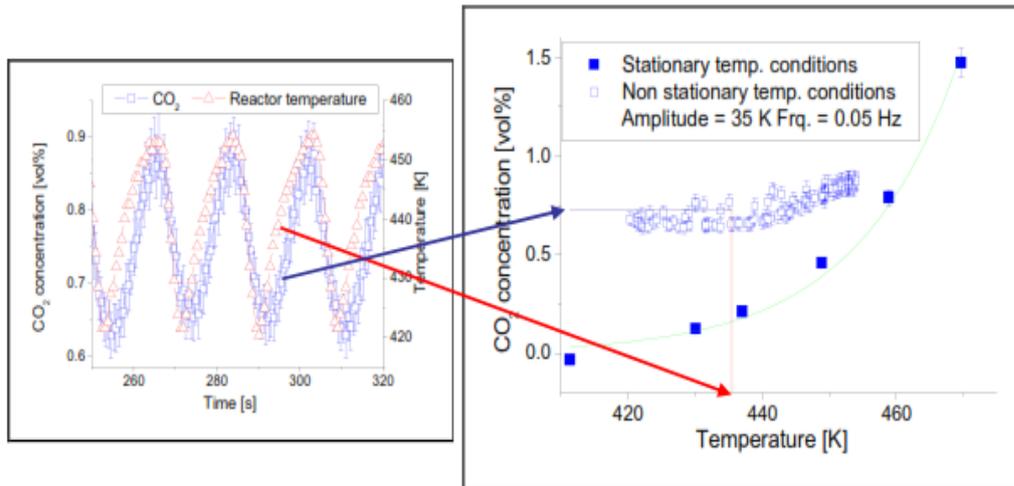
Figure 6. Conversion comparison between stationary system and forced unsteady state system by CO oxidation **[7]**

1.1.1.1.3 Catalyst Deactivation/Regeneration

Catalyst deactivation by poisoning, metal volatilization and sintering are very important problems [8, 9, 10]. These situations are especially very problematic at high temperature conditions.

Although temperature at the center of the catalyst bed can reach higher values for RFR than steady state values, the temperature regulation at both sides of the reactor in RFR provides an extra unique advantage which is a balance between reaction rate (conversion) and catalyst deactivation. Higher conversion can be obtained in RFR due to the higher temperature plateau, while catalyst deactivation rate is not accelerated by temperature regulation. Conversion, selectivity, working temperature and catalyst deactivation comparison between steady state reactors and RFR can be seen at Figure 7 for Pt catalyst, Rh catalyst and Ir catalyst. The conversion graphs which have dark sphere or triangle show that conversion amount is not decreasing sharply for RFR; however, the others which have empty sphere or triangle show that conversion amount is decreasing sharply for steady state reactor [11].
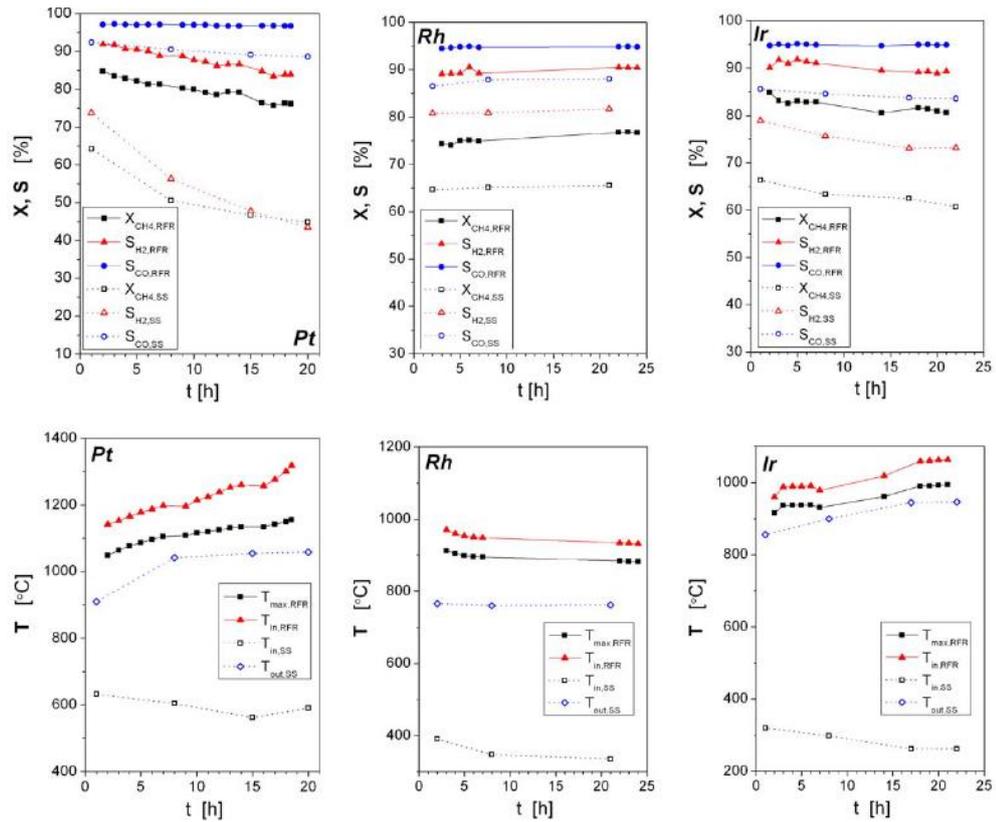
Figure 7. Conversion, selectivity, working temperature and deactivation comparison between steady system and RFR system for Pt catalyst, Rh catalyst and Ir catalyst **[11]**

1.1.1.1.4 Cost Reduction

In addition to the three advantages given above, another advantage of RFO systems is the elimination of a heat exchanger from the process design. Therefore, RFO reactors eliminate the need for intercooling stages with serial reactors. As a result, the final advantage of RFR is making cost reduction for industrial systems. A VOC incineration system was designed and constructed by Haldor Topsoe, Boreskov Institute of Catalysis and Monsanto Enviro-Chem Systems. The cost comparison between this catalytic reversed process and three other common processes show in Table 1 [12].

Table 1. Cost comparison of different VOC incineration reaction systems [12]

Method	Capital Cost	Operating Cost
Catalytic, recuperative	1	1
Thermal, recuperative	1.8	2
Thermal, regenerative	1.6	0.5
Catalytic, regenerative (Catalytic Reversed Process)	1	0.2

Table 1 shows arbitrary cost comparison with respect to catalytic, recuperative method. It shows that the oldest process type (thermal, recuperative) is the most expensive one in both capital cost and operating cost values. While catalytic, recuperative processes can be alternatives with respect to capital cost and thermal, regenerative process can be an alternative with respect to operating cost, catalytic reversed process gives considerable advantages for both capital and operating cost.

1.1.1.2 Industrial Applications of RFR

There are various commercialized RFO systems:

1. Catalytic incineration of NO_x compounds in industrial waste gases [13, 14, 15]
2. SO_2 oxidation after nonferrous metal smelters [13, 16, 17]
3. Selective NO_x reduction [18, 19]

   There are also reactor designs which can eliminate heat exchangers for reversible reactions like SO_2 oxidation, methanol synthesis and ammonia synthesis [5, 13].

1.1.2 Loop Reactor

Loop reactors (LR) work by changing the feed point of the process or changing the reaction in the reactor periodically. Figure 8 shows the basic LR configuration which changes feed point and Figure 9 shows changing the reaction in the reactor ones.
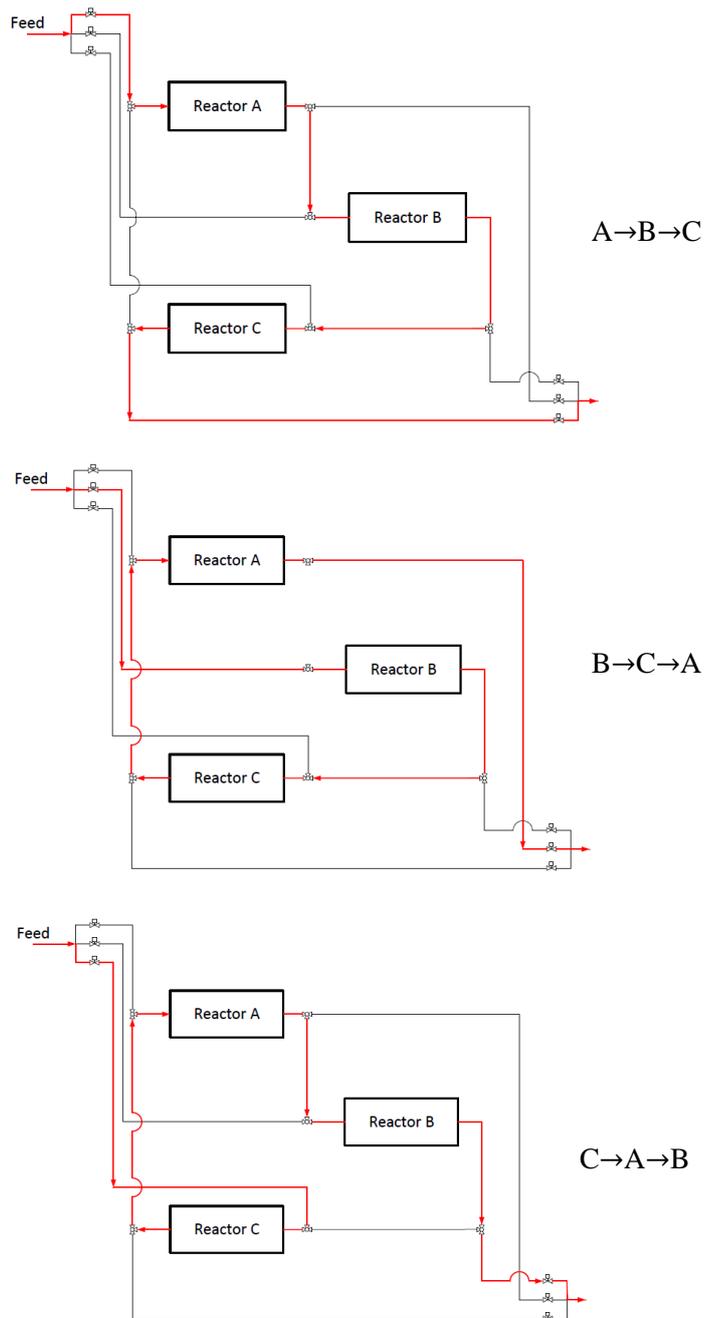
Figure 8. Feeding point changing periodically from Reactor A to Reactor C. Top: path A→B→C, middle: B→C→A, bottom: path C→A→B. [8]

In the basic LR configuration, which changes feeding point, reactors are connected to each other in serial. Feeding stream goes into reactor A at first. After it is gone out of reactor A, the stream is gone into reactor B and reactor C respectively. The stream follows three different paths if there are 3 reactors. These are A-B-C, B-C-A and C-A-B paths.
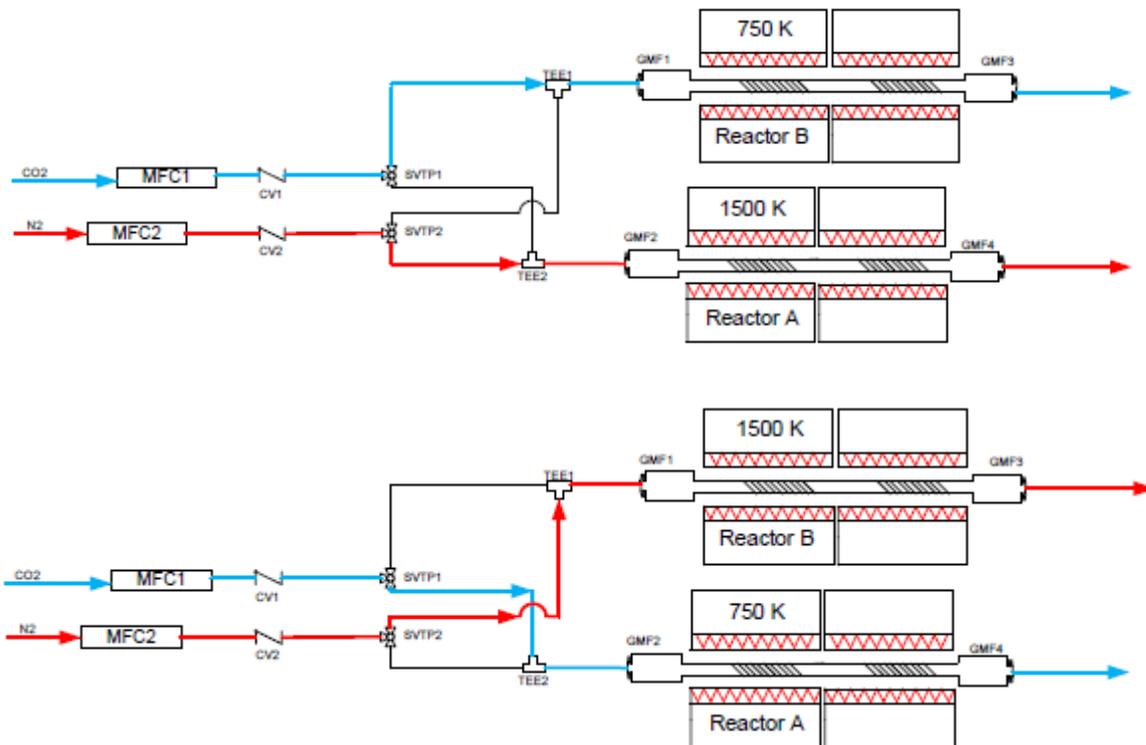
Figure 9. LR configuration with changing the reaction in the reactors

Reactors are parallel in LR configuration with changing the reaction in the reactors. There are two reactors in the basic configuration of that. In the figure above, N_2 is fed into reactor A of which temperature is 1500 K and CO_2 is fed into reactor B of which temperature is 750 K.

After some time, the ways of three way valves are changed. Reactor A is fed by CO_2 and reactor B is fed by N_2. Due to the fact that the reactions can be occurred, the temperature of the reactors is also changed.

There are two main advantages of LR:

1. Lower heat loss
2. Lower catalyst deactivation

The main disadvantage of this type of reactor system is the complexity of controlling the system. There should be many valves, lines etc.

1.1.2.1 Advantages of LR

1.1.2.1.1 Decreasing Heat Loss

The main advantage of LR is reduced heat loss. By this advantage, LR can reach temperatures higher than even flow reversal reactors. The two main reasons of decreasing heat loss are having feed dispersion and having no boundaries. Heat loss by conduction can be eliminated because there are no edges by making good loop design.

1.1.2.1.2 Decreasing Catalyst Deactivation

Catalyst deactivation is an important problem for reaction systems. Hot spots can occur in catalyst bed especially in exothermic reactions. These hot spots decrease the life of the catalyst. In LR systems, hot spot patterns rorate. So, it is averaged for whole reactor system. Because of that, catalyst life can be longer for LR systems [20].

1.2 Temperature Programmed Desorption (TPD)

Temperature Programmed Desorption (TPD) is a technique in which the behavior of adsorbate can be explored. It can be also called Temperature Programmed Reduction (TPR), if a material is reduced by adsorbing or desorbing a molecule. In this technique, an atomic or molecular gas is adsorbed on the surface. Then, this surface is heated with heat ramp giving a linear temperature=time profile. The increase in temperature causes the adsorbed molecules to desorb. The desorbed gas can be monitored by a mass spectrometer, TGA, TCD etc. In result, a plot of the desorbed gas amount vs. sample temperature is obtained. This plot is called the TPD spectrum. Generally, there are three types of TPD spectra;

1) TPD spectra of samples pretreated differently.
2) TPD spectra of different materials in comparison with each other.
3) TPD spectra of different molecules from same sample.

1.2.1 What Can Be Learned from TPD Analysis?

Basically, there are four different phenomena which can be learned from TPD analysis [21];

1) Heat of adsorption from reversible/non-dissociative adsorption and desorption processes
2) Quantitative coverage information from dissociative and non-dissociative adsorption processes
3) Energetic information about phase transition, interadsorbate interaction, multiple adsorption sites
4) Kinetic information about desorption process

1.2.1.1 Heat of Adsorption Analysis

The temperature dependence of adsorbate coverage can be obtained from the adsorption isotherms by Clausius-Clapeyron equation.

If it is assumed that equilibrium is achieved for the adsorbed particles (N_{ads}) on the surface and in vapor phase, (N_{surf}), it means that there is an equilibrium between chemical potentials of the both phases of particles ($d\mu_{ads}=d\mu_{gas}$). If $\theta=N_{ads}/N_{surf}$ and volume of condense surface phase, the equation is become;

$$\left(\frac{\partial lnp}{\partial T}\right)_\theta = \frac{q_{isost}}{RT^2} \tag{1.1}$$

where q_{isost} is isosteric heat of adsorption and its equation;

$$q_{isost} = (\partial H/\partial\theta)_T \tag{1.2}$$

If the equilibrium is defined by a constant pressure $\emptyset$ at the surface instead of constant surface coverage θ, Clausisus-Clapeyron equation becomes;

$$\left(\frac{\partial lnp}{\partial T}\right)_\emptyset = \frac{q_{eq}}{RT^2} \tag{1.3}$$

Where q_{eq} is equilibrium heat of adsorbtion and its equation;

$$q_{eq}(\emptyset) = \int_0^\emptyset dH_T(\emptyset')d\emptyset' \tag{1.4}$$

1.2.1.2 Quantitative Coverage Analysis

Calculating the adsorption molecule amount from TPD data is possible. If there is calibration data for the detector that is analysing desorbed molecules, it is easy to quantify the area under the curve in TPD spectrum as the amount of the desorbed molecule. The amount of the desorbed molecule is considered to be the same with the quantitative coverage amount of adsorbed molecule in the absence of multiple interactions.

1.2.1.3 Multiple Adsorption Site and Interadsorbate Interaction Analysis

One molecule can be bound to different sites of a surface. It also can be different binding types (different binding strenghts); so the same molecule can have different activation energies of desorption.

It is possible to recognize this different binding sites or activation energies from TPD data. If there is more than one peak in a TPD data of one molecule, each peak corresponds to a different activation energy of desorption. Different activation energies indicate different binding energies between the molecule and the surface. In the next section the relationship between the desorption temperatures and the activation energy of desorption will be presented.

1.2.1.4 Kinetic Information of Desorption Process

If the rate of desorption shows an Arrhenius-type behaviour;

$$\frac{r_d}{N_s} = -\frac{d\theta_A}{dt} = k_\circ \theta_A^n \exp(-\frac{E_A}{kT}) \tag{1.5}$$

Where r_d is the rate of desorption of species A in molecule/cm^2; N_s is concentration of surface sites in number/cm^2; θ_A is the coverage of species A; t is time; n is the order of the desorption reaction; $k_\circ$ is frequency factor; E_A is the activation energy of desorption; k is Boltzmann's constant; and T is temperature.

As mentioned above, temperature increases linearly in TPD analysis. So;

$$T = T_\circ + \beta_H t \tag{1.6}$$

Where $T_\circ$ is the initial temperature and β_H is the heating rate. If the equation 1.5 is combined with equation 1.6.

$$\frac{r_d}{\beta_H N_s} = -\frac{d\theta_A}{dT} = \frac{k_0}{\beta_H} \theta_A^n \exp(-\frac{E_A}{kT}) \tag{1.7}$$

When equation 1.7 is examined, it is clear that E_A, k_0, β_H and θ_A (if n$\neq$ 1) affects peak desorption temperature. k_0, β_H and n effects to peak shape. θ_A effects peak magnitude. The order of the desorption process, n, influences the shape of the desorption curve. So, one can determine the desorption order from the shape and the activation energy by the peak temperature.

1.2.1.4.1 Zero-Order Desorption

This type of desorption kinetic implies that desorption rate does not depend on coverage and increases exponentially with T.
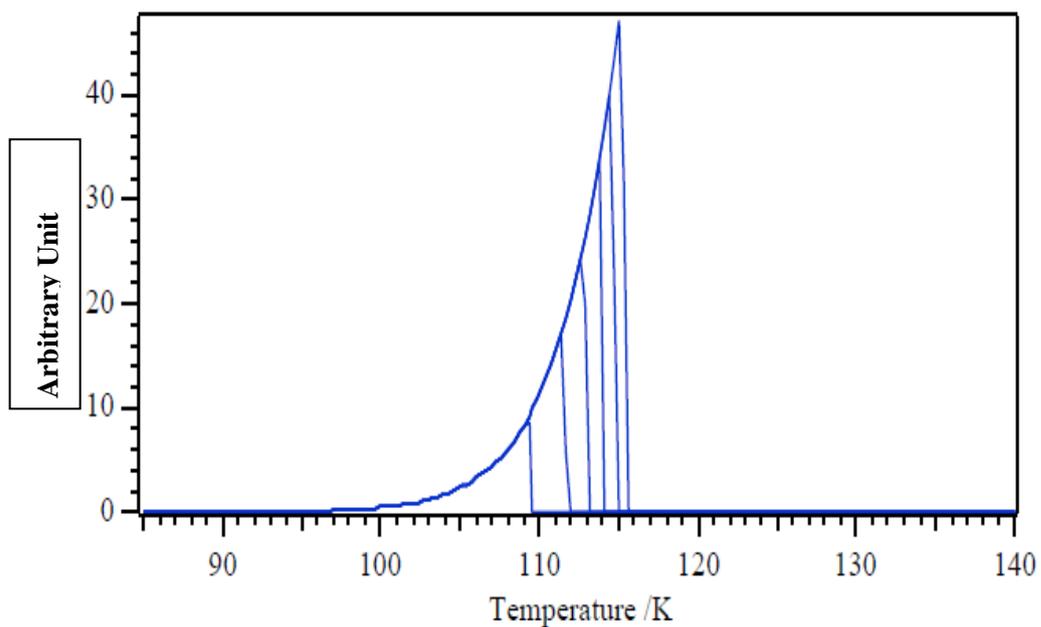
Figure 10. Zero-order TPD plot. E_A=30 kj/mol; $k_\circ$=1x10^{28}; β_H=1.5 K/s; θ_A=1.6x10^{13} cm^{-2}

One can understand that desorption rate increases until all molecules are desorbed and temperature of peak desorption rate increases with increasing θ_A. This process is typical of sublimation or evaporation.

1.2.1.4.2 First-Order Desorption

This type of desorption kinetic implies that desorption rate is proportional to instantaneous coverage and desorption peak have a balance of θ_A and exp($-E_A$/kT) terms.
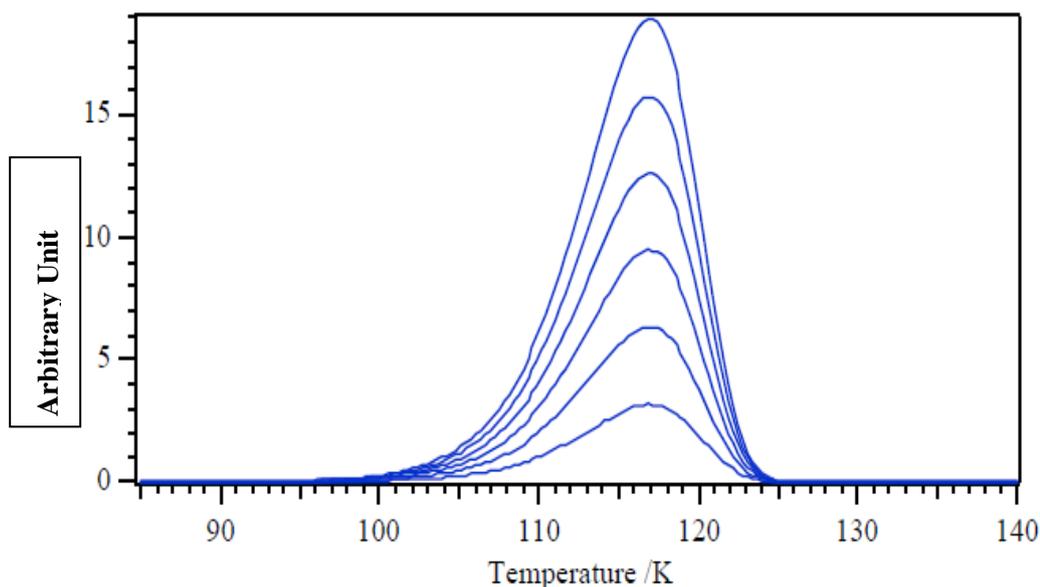
Figure 11. First-order TPD plot. E_A=30 kj/mol; $k_\circ$=1x10^{13}; β_H=1.5 K/s; θ_A=1.6x10^{13} cm^{-2}

As seen in Figure 11, the peak temperature does not change with increasing θ_A, characteristic peak shape is asymmetric.

1.2.1.4.2 Second-Order Desorption

This type of desorption kinetic implies that desorption rate proportional to instantaneous coverage square and desorption peak have a balance of θ_A and exp(-E_A/kT) terms.

As seen in figure 12, the peak temperature of desorption is decreasing with increasing θ_A and peak shape characteristic is nearly symmetric.

1.2.2 Instruments for TPD Analysis

The typical TPD set-up should consist of a furnace, a temperature controller, and a cooling system if sub-ambient temperatures are also needed in the experiments. Flow rate of the gases going through the system is adjusted by mass flow controllers and needle valves. Finally the effluent gases can be analyzed by a thermal conductivity detector (TCD) if there is only one desorption product. In the case of multiple products a mass spectrometer (MS) is desirable.
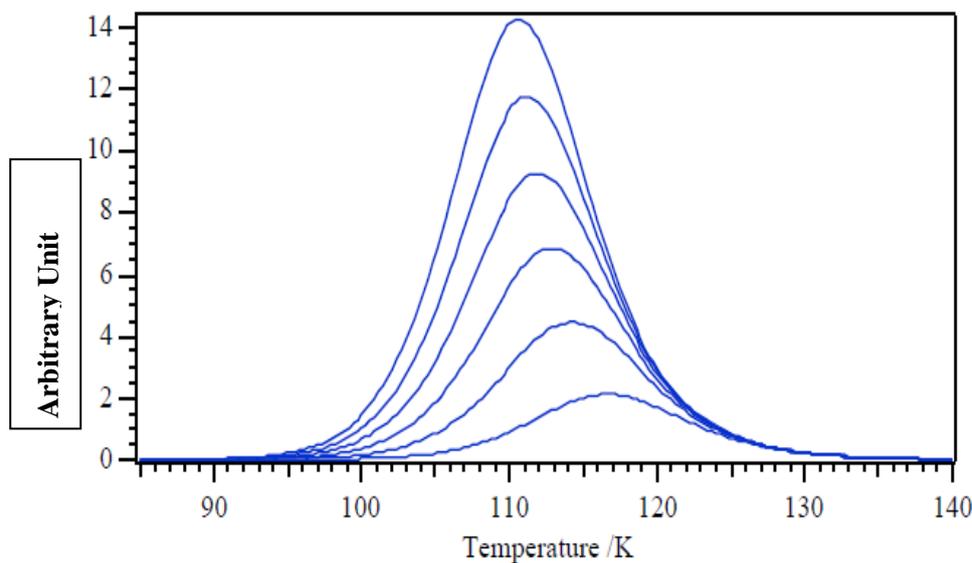
Figure 12. Second-order TPD plot. E_A=30 kj/mol; $k_\circ$=1x10^{-1}; β_H=1.5 K/s; θ_A=1.6x10^{13} cm^{-2}

There are two main advantages of using TCD;

1) Calibrating and using TCD is very easy.
2) Using TCD is preferable for the systems that need analog outputs.

However, TCD is appropriate only for binary systems. If there are more than one desorbing materials, it is not possible to understand which peak for which desorbing material from TCD data. MS provides good monitoring for outlet gas composition. Due to the fact that one can monitor a lot of different molecules in a gas composition with MS, MS is preferred in most of the TPD experimental systems.

There are also some special instruments to make TPD/TPR analysis. Micromeritics has 27xx series for TPx analysis. There are some basic advantages of this series;

- Dead volume is very little in this instrument
- TCD in these instruments is very sensitive. It is possible to monitor very low concentrations of desorbed molecules.
- Instruments can be operated without any PC.

Main disadvantage of these instruments is all the valves and process equipment of the system are manual. Micromeritics also has an instrument is called Autochem. Autochem has all the advantages of 27xx series, in addition to them; all the process equipments of it are automatic. It only should be programmed for desired analysis. Disadvantage of this instrument is its price. It is an expensive instrument.

Hiden Analytical also has a special instrument called IGA. It is also suitable for TPx experiments. Basic advantage of IGA is that one can make BET, TPD, TPR and TPO experiments by loading only one sample. Disadvantages of this instrument are price and difficult sample loading. Although It is very useful for making a lot of experiments with one sample, it is not appropriate to make TPD with a lot of different samples.

1.2.3 Steady State Isotopic Transient Kinetic Analysis (SSITKA)

Development of this technique was started in 1978 with a work of Happel [22]. After that Bennett [23] and Biloen [24] continued working on this topic in 1982 and 1983 respectively. Detection of isotopic labels in flowing stream thorough the reactor versus time is principle of this technique. One of the important things about this technique is that isotopic labeling should be one of the reactant species and it should be given by step change into the reactor feed. Operation should be isothermal and isobaric and it is also very important that concentration of reactant and product should be same before and after making step change to give isotopic labels into the system. A basic experimental setup to make SSITKA experiment is shown in Figure 13.
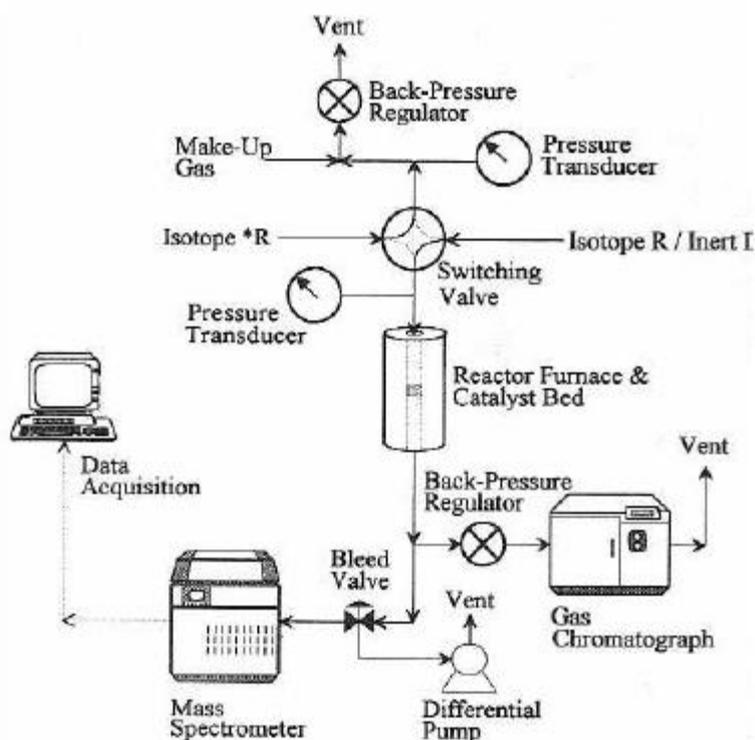
Figure 13. Basic reaction system for SSITKA experiments [22]

There are two pressure transducers and two back pressure regulator in this system. One of transducer and one of back pressure regulator are at the inlet part of the system to arrange pressure of inlet gas. Other ones are at the outlet part of the system to arrange pressure of outlet gas. System should be isobaric; so, back pressure valves arrange inlet and outlet gas to same pressure amount. There is also one switching valve at the inlet part to make step change of inlet gas and isotopic labeled gas stream. Although, there can be a gas chromatograph (GC) to monitor different gases in outlet stream, MS is a must in such a system to be able to monitor isotopic labeled gas. Figure 14 shows typical normalized isotopic transient responses.
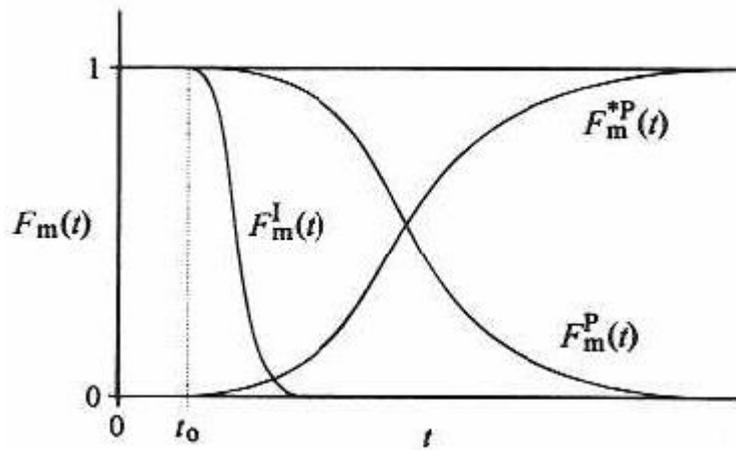
Figure 14. Typical normalized isotopic-transient responses **[25]**

Where $F_m^{*P}(t)$ is step-input of the product for new isotopic label, $F_m^{P}(t)$ is step-decay of the old isotopic label and $F_m^{I}(t)$ is inert-tracer for determination of gas-phase holdup. The relationship between step-input and step-decay is

$$F_m^P(t) = 1 - F_m^{*P}(t) \tag{1.8}$$

By performing this type of measurement, it is possible to understand the accumulating species on the surface without disturbing the dynamics of the system.

CHAPTER 2

LITERATURE SURVEY

2.1 Metal Oxides for Oxidation – Reduction Reactions

Redox catalysts are catalysts which can be reduced and oxidized in a reaction simultaneously or one by one. The general description of redox processes on metal oxide can be shown as below [26].

$$Cat\text{-}O + Red \longrightarrow Cat + Red\text{-}O \qquad 1$$

$$Cat + O_x\text{-}O \longrightarrow Cat\text{-}O + O_x \qquad 2$$
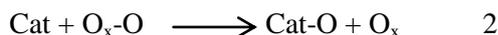
This oxidizing mechanism by metal oxide is commonly accepted mechanism. This mechanism was proposed by Mars and van Kravelen in 1950s [27]. Substrate in the reaction is oxidized by taking oxygen atom from metal oxide but not gas phase oxygen according to this mechanism. Gas phase oxygen has a role of oxidizing again the metal oxide. Even though it was shown that the first step of oxidizing hydrocarbons is started with abstraction of proton from hydrocarbons [28 - 34], for many reactions it is confirmed that metal oxides give their oxygen atom and re-oxidized again with gas phase oxygen. This situation makes metal oxides as oxygen source and also makes reduced metal oxides as oxygen scavengers from any oxygen containing material.

2.1.1 Reduction and Oxidation of CeO_2 and CeO_2 Mixed Oxides

In 1990s, research about CeO_2 metal oxide had started to accelerate. It was shown that CeO_2 formed easily by calcining cerium salts in oxygen containing atmosphere [35 – 39]. Kibourn, B. T. showed that cerium has highest free energies of formation for a metal oxide [40]. Finally, Gandhi et al. showed ceria has very good oxygen storage/release capacity (OSC/ORC) [41].

In addition to all these studies, oxygen abstraction from ceria is widely studied in the literature. Lin, S. S. et al. studied catalytic wet air oxidation of phenol by using ceria catalysts [42]. According to this work, they showed that CeO_2 that pretreated with O_2 can give higher amount of O_2 than not pretreated one. Chen, I. P. et al. worked on optimal ceria catalyst to oxidize phenol [43]. They performed O_2 TPD experiments with commercial ceria

and ceria mixed oxides and they showed that ceria mixed oxides can give their oxygen at lower temperatures than commercial ceria.
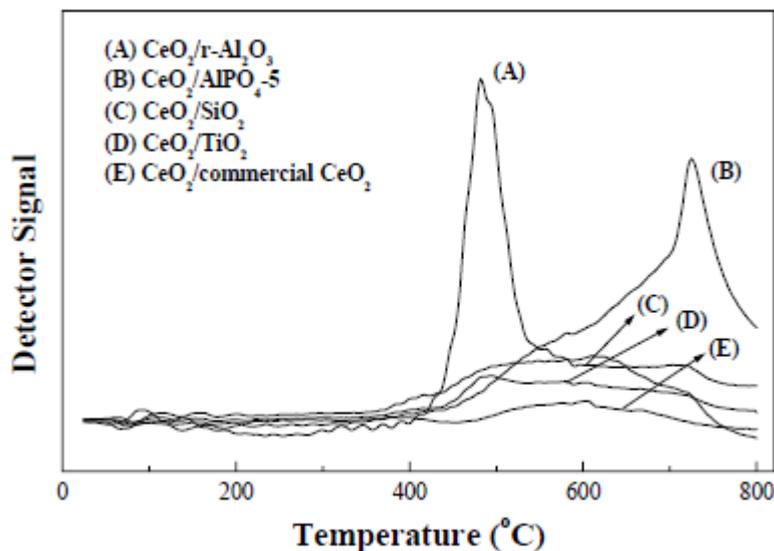
Figure 15. O_2 TPD spectra of various supported CeO_2 catalysts [43]

All the researches about using ceria as oxygen pump due to its high oxygen storage capacity (OSC) and oxygen release capacity (ORC) give another direction to researches in order to use this material for reducing CO_2 and H_2O. By this way, H_2 production and syngas production can be possible from waste gas of some industrial processes. Sharma, S. et al. reported to oxidize reduced ceria by CO_2 [44]. To prove CO_2 reduction over ceria, they gave He into the reactor and gave two CO pulses. After the first pulse, they can see CO_2 pulse due to the fact that ceria oxidized CO; however, after second pulse they can not see any CO_2 pulse because ceria gave its all kinetically active oxygen atoms to oxidize first pulse of CO. After that, they gave CO_2 pulse this time and they saw CO peak from mass spectrometer. It is shown that unstable Ce_2O_3 molecule stole oxygen of some CO_2 molecules. Then, they gave CO pulse again and saw again CO_2 peak. This CO_2 peak is evidence which shows some of Ce_2O_3 molecules turned to CeO_2 molecules while CO_2 gas passed over them.

Chueh, W.C. et al. also made an interesting research with CeO_2 [45]. They used a solar concentrator to heat ceria catalyst. After heating ceria to high temperatures at around 1500^0C, ceria gave its active oxygen atoms. After that they gave CO_2 into the reactor and they took CO from the outlet of the reactor. They did same thing with H_2O also and they took H_2 this time.

20
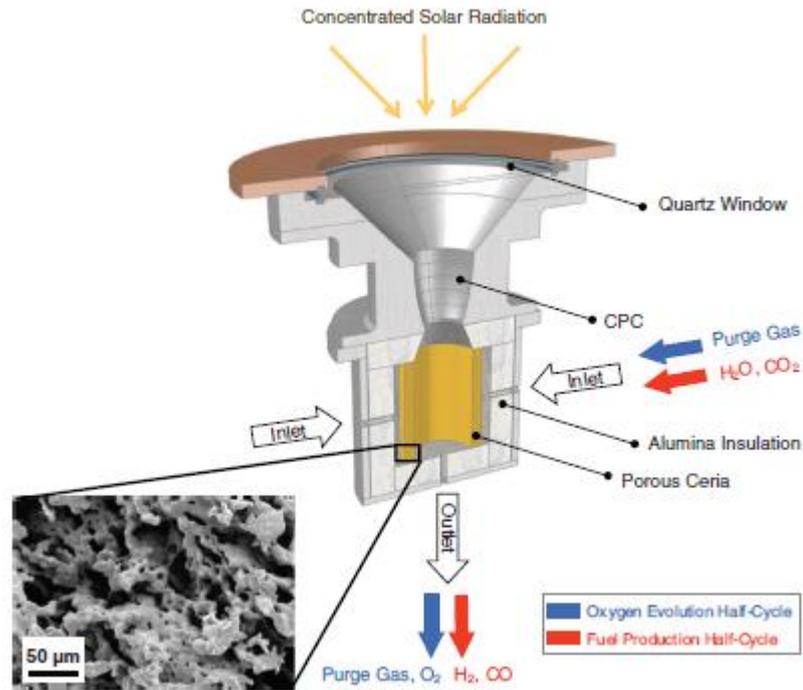
Figure 16. H_2O and CO_2 reduction system with Ceria that is heated by solar concentrator[45].

2.1.2 Comparison of O_2 TPD Between Pt/CeO_2 and CeO_2

Decreasing the oxygen desorption temperature of CeO_2 is very important. Platinum is a well known precious metal to make desorption of oxygen easier for catalysts. Gaillard studied oxygen desorption difference between CeO_2 and Pt/CeO_2 [46]. This work showed that platinum on the surface of CeO_2 lowered the oxygen desorption temperature of the catalyst.

Another important thing about oxygen desorption of the catalyst is the surface area of CeO_2. Uner et al. studied the effect of the surface area for oxygen desorption of the catalyst by CO oxidation reaction [47]. This research showed that while the surface area of Pt/CeO_2 from commercial CeO_2 is just 2.7 m^2/g, the surface areas of catalysts, of which CeO_2 supports produced from $CeCl_3.XH_2O$ and $Ce(C_2H_3O_2).1.5H_2O$, are 16.2 m^2/g and 64.6 m^2/g respectively. The catalyst with highest surface area gave highest conversion at lower temperature which means the catalyst gave it oxygen at lower temperature. Pt dispersion of the catalyst is another important point. In the same study, catalyst elutriation with hot water is very important to increase dispersion percent since this process helps getting rid of chlorine molecules over the catalysts.
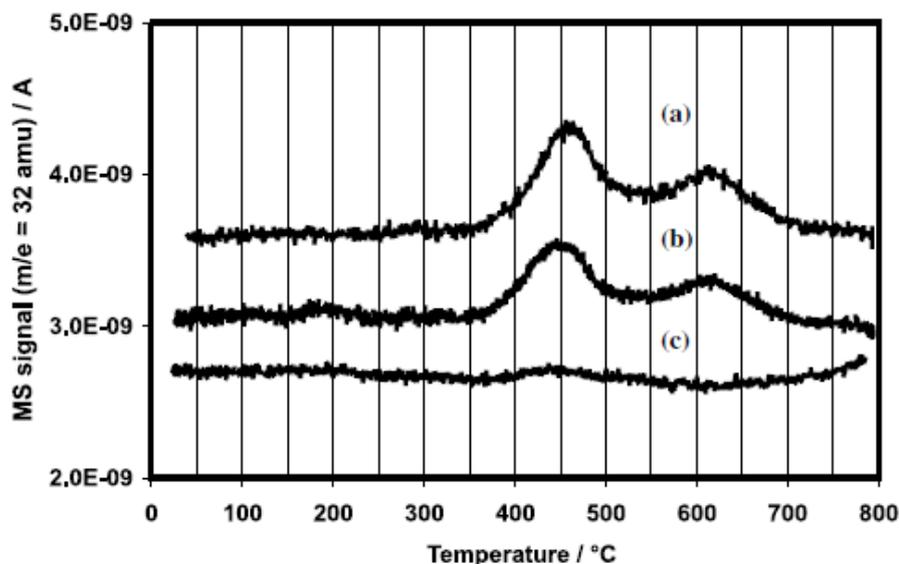
Figure 17. Oxygen TPD spectra of (a) Pt/CeO$_2$ with CO$_2$ adsorption, (b) Pt/CeO$_2$ without CO$_2$ adsorption and (c) CeO$_2$ [46]

2.2 Temperature Programmed Desorption

Catalyst characterization is an important process to get information about catalysts. Temperature programmed desorption is one of most important technique for catalyst characterization. Reactants are adsorbed on the catalyst surface, and then products are desorbed from the surface in a reaction. Because of that, it is very important to know kinetic and energetic information of these situations.

In TPD method, solid that absorbs gas molecules is heated with linear temperature rise. Outlet gas of the system is monitored continuously. By this way, desorption amount and temperature of a molecule can be detected. Area under the curve of intensity of desorbed molecule gives desorbed molecule amount and desorption temperature gives the information about the strength between absorbed molecule and surface. Redhead [48] first described that TPD can be used as a quantitative analytical tool. In 1963, Amenomiya and Cvetanovic [49] showed that this technique can be used to examine high surface area catalysts under carrier gas at atmospheric pressure. With these two different methods of TPD, it is possible to investigate the relationship between material and pressure gaps in heterogeneous catalysts. Falconer and Schwarz [50], Lemaitre [51] and Tovbin [52] reviewed theory and application of TPD. Gorte [53] suggested that TPD can be a good tool to identify reaction pathways and site densities. One can be able to make a comparison of adsorption capacity, metal surface area or metal dispersion on the catalyst with total desorbed molecule amount data of different catalysts. Arena [54] also investigated surface acidity of some catalysts by NH$_3$-TPD.

Although TPD is generally used for qualitative analysis, quantitative kinetic and energetic analysis also can be made by TPD data. Falconer [55] studied desorption rate isotherm method. Arrhenius plot methods are investigated by Rudzinski [56]. Rudzinski showed energetic heterogeneity of surface and their limitations. The starting point of Rudzinski is given in equation (2.1)

$$\frac{d\theta}{dt} = K_a P (1-\theta)^s e^{-\epsilon_a/kT} - K_d \theta^s e^{-\epsilon_d/kT} \qquad (2.1)$$

Another method to extract kinetic parameters from TPD data is nonlinear regression which is based on model fitting. This method was introduced by Russell and Ekerdt [57]. In 1980s, several studies were made to find desorption kinetics of porous samples [58, 59, 60]. While Ibok and Ollis [61] presented modified Weisz, a more accurate mathematical description for desorption kinetics of porous catalyst was put by Herz [62].

$$-\frac{d\theta}{dt} = [1 - (1+Z)(1-\theta)]W^{(Z)} + Z1 - \theta W^{(Z)} \qquad (2.2)$$

Where;
θ is surface coverage
Z is the number of neighboring sites
W is the transition probability per unit time for such adsorbates

A simulation model was established by Rieck and Bell [59]. They put adsorption and desorption kinetics and reactor model in this study. Both CSTR and multiple CSTRs (packed bed behavior) were modeled. Jansen [62] performed a Monte Carlo simulation of TPD spectra. The important thing is attractive lateral interactions are taken into account in this work. Wang et al. [63] made micro kinetic simulation of TPD recently.

In TPD analysis, MS is used generally to detect more than one molecule continuously. However, TCD can also be used to monitor outlet flow. The problem is mix gases cannot be monitored with TCD. This type of detector is appropriate to detect only one gas in a flow. Because of that reason, choosing reference (carrier) gas is very important in TCD. Thermal conductivity difference of reference gas and desorbed gas should be significant. Fadoni and Lucarelli [64] put a work for this phenomenon.

Another important thing about adsorption/desorption experiments is choosing adsorptive material. There are some important properties should be taken into consideration to choose adsorptive material. These factors are; [64]

- Gas dissolution amount in the metal
- Adsorption on the support
- Minimum equilibrium time
- Reaction between gas and metal
- Purity of gas

Table 3 shows general classification of the adsorption type of some metals and gases.

Table 2. Detection of some gases in relation to different carriers by TCD [64]

Gas	Main Use	Thermal Conductivity (*)	Detectable reactive gases
He	Carrier	3363	O_2, CH_4, CO, CO_2, SO_2, H_2S, NH_3, NO, N_2O
Ar	Carrier	406	H_2
N_2	Carrier	580	H_2
H_2	React./ Carrier	4130	CO, CO_2
O_2	React.	583	-
CH_4	React.	720	-
CO	React.	540	-
CO_2	React./ Carrier	343	H_2
SO_2	React.	195	-
H_2S	React.	327	-
NH_3	React.	514	-
NO	React.	555	-
N_2O	React.	374	-

(*) Determined at 273K, values $.10^7$ (cal/cm.s.K).

Table 3. Adsorption type of metals [65]

Metals	Dissociative Form					Associative Form				
Gases	H_2	N_2	O_2	NO	CO	H_2	N_2	O_2	NO	CO
Hg, Ta, Zr, Nb, W, Ti, V, Mn, Cr, Mo	+	+	+	+	+	-	-	-	-	-
Fe, Re	+	+	+	+	+	-	-	-	+	+
Ni, Co, Tc	+	+	-	+	+	-	-	-	+	+
Os, Ir, Ru, Pt, Rh, Pd	+	+	-	+	-	-	-	-	+	+

2.2.1 Temperature Programmed Desorption of Oxygen

Oxygen TPD from metal oxide has been a hot topic since 1980s. Iwamoto et al. [66] investigated oxygen desorption from Nickel Oxide in 1976. They showed that there are four

different adsorption/desorption sites. Two of them (β and γ) have strong desorption peaks whereas the others (α and δ) have weak desorption peaks. Iwamoto et al. [67] also investigated oxygen desorption from various transition metal ion-exchange Y-type zeolites in 1976. They made experiments with Cu^2Y, Co^2Y, Mn^2Y, NaY and Ni^2Y. Oxygen desorption amounts of these catalysts were calculated from the area under the curves of TPD spectra. Results were found as 1.08 cm^3g^{-1}, 3.76 x 10^{-2} cm^3g^{-1}, 3.44 x 10^{-2} cm^3g^{-1}, 2.14 x 10^{-2} cm^3g^{-1} and 1.58 x 10^{-2} cm^3g^{-1} respectively. In addition to these, same group investigated oxygen desorption from different metal oxides. Table 4 shows results of these desorption experiments.

Table 4. Oxygen TPD results of some metal oxides [68]

Metal Oxides	Desorption Temperature (^{0}C)	Oxygen amount cm^3/m^2
V_2O_3	-	0
MoO_3	-	0
$Bi2O_3$	-	0
WO_3	-	0
$Bi_2O_3.2MoO_3$	-	0
Cr_2O_3	450	2.13×10^{-2}
MnO_2	50, 270, 360, 540	6.54×10^{-2}
Fe_2O_3	55, 350, 486	4.05×10^{-3}
Co_3O_4	30, 165, 380	3.30×10^{-2}
NiO	35, 335, 425, 550	1.12×10^{-2}
CuO	125, 390	1.42×10^{-1}
Al_2O_3	65	2.05×10^{-4}
SiO_2	100	2.99×10^{-5}
TiO_2	125, 190, 250	5.52×10^{-5}
ZnO	190, 320	2.45×10^{-4}
SnO_2	80, 150	2.11×10^{-3}

2.2.2 Temperature Programmed Desorption at Cryogenic Temperature

Temperature programmed desorption can be also done at cryogenic temperatures. For this purpose, some molecules have very low boiling points like liquid nitrogen, liquid helium, liquid carbon dioxide etc. are used to cool the sample. These experiments need some special designed systems to dose these cooling mediums into the system and control the temperature

and heating rate of the system. Haegel et al. [69] designed a system to make large number of TPD analysis at cryogenic temperatures (Figure 19). In this system, there is a buffer reservoir above the chamber. This special designed reservoir allows using any over pressured liquid nitrogen vessel only if this overpressure is enough to lift liquid nitrogen to the buffer reservoir. By this way, the vessels can be changed without interrupting measurement.
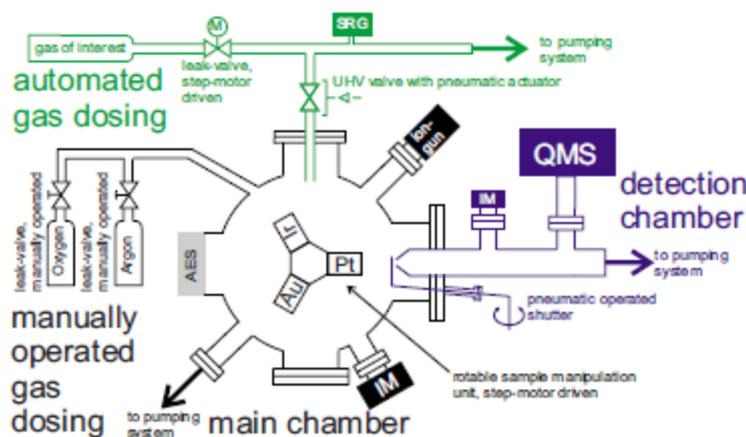
Figure 18. An example of a system to make TPD at cryogenic temperatures [69]

Traditional TPD analysis is not suitable to examine physisorbed molecules on surface. Temperature programmed desorption method is used at cryogenic temperatures to detect especially weak bonds between adsorbed molecules and surface. Choi et al. [70] investigated TPD of H_2 from molybdenum nitride thin films. Although there is a desorption peak at 700 – 800 K, they found that there is also a peak at 370 K and H_2 is adsorbed at 270K. Pirolli and Teplyakov [71] studied kinetics and energetics of vinyltrimethylsilane (VTMS) adsorption and desorption on Si(100). Guenard et al. [72] showed methanol is molecularly adsorbed in the monolayer at cryogenic temperatures and also dissociative adsorption of alcohols form alkoxide intermediate on metal oxides. Artsyukhovich et al. [73] examined oxygen adsorption/desorption dynamics on Pt(111) by TPD experiments starting from 20 K up to 1000 K. They showed that first physisorbed monolayer is occurred at 20 K whereas it alters to chemisorbed form at 30 – 40 K. They also proved that chemisorbed O_2 is desorbed or dissociated to O atoms between 100 – 160 K.

In summary, TPD should be done at cryogenic temperatures to detect physisorbed molecules that have weak bonds. Traditional TPD analys is not enough to detect such situation.

CHAPTER 3

MATERIALS AND METHODS

3.1 Materials

There are three different chemicals to synthesize supports and catalysts that are used in experiments. These are γ-Al_2O_3 (Johnson – Matthey), $Ce(C_2H_3O_2).1.5H_2O$ (Johnson – Matthey) and $Pt(NH_3)4Cl_2.H_2O$ (tetraamine platinum-II-chloride, Johnson – Matthey). Gases used in experiments are N_2 (99.9%), CO_2 (99.9%) and O_2 (99.9%) which was purchased from Linde.

3.2 Support and Catalyst Preparation

3.2.1 Synthesis of Al_2O_3- CeO_2 Support with Incipient Wetness Method

Al_2O_3-CeO_2 catalysts with 10 wt% CeO_2 are prepared by incipient wetness method. Mixed oxide support is prepared from $Ce(C_2H_3O_2).1.5H_2O$ (Johnson – Matthey). Appropriate amount of material is dissolved in $1 - 2$ ml water/g Al_2O_3. Al_2O_3 is purchased from Johnson – Matthey. Finally, the slurry of the two metal oxides is dried at 120 °C in an air flow and calcined at 600 °C.

3.2.2 Synthesis of Pt/CeO_2 Catalyst with Incipient Wetness Method

1 wt % Pt/CeO_2 catalysts are prepared by incipient wetness method. CeO_2 support is prepared from $Ce(C_2H_3O_2).1.5H_2O$ (Johnson – Matthey). $Ce(C_2H_3O_2).1.5H_2O$ is calcined 600^oC for 4 h to get pure CeO_2 support. Platinum solution for the catalyst is prepared by dissolving appropriate amount of $Pt(NH_3)_4Cl_2.H_2O$ (tetraamine platinum-II-chloride, Johnson–Matthey) in 1 -2 ml water/g support. This solution is impregnated over the support. The catalyst dried at room temperature overnight and at 120^oC for 4 h. Then, the catalyst is calcined at 450 ^oC for 4 h. Finally, catalyst is washed with hot water to eliminate residual chlorine and dried at 120 ^oC overnight.

3.2.3 Synthesis of Pt/Al$_2$O$_3$-CeO$_2$ Catalyst with Incipient Wetness Method

1 wt % Pt/Al$_2$O$_3$-CeO$_2$ catalysts are prepared by incipient wetness method. Platinum solution for the catalyst is prepared by dissolving appropriate amount of Pt(NH$_3$)$_4$Cl$_2$.H$_2$O (tetraamine platinum-II-chloride, Johnson–Matthey) in 1 -2 ml water/g mixed oxide support. This solution is impregnated over the support. The catalyst dries at room temperature overnight and at 120°C for 4 h. Then, the catalyst is calcined at 450 °C for 4 h. Finally, catalyst is washed with hot water to eliminate residual chlorine and dried at 120°C overnight.

3.2.4 Synthesis of Pt/Al$_2$O$_3$-CeO$_2$ Catalyst with Polyol Method

100 ml ethanol is put into a reflux glass. Appropriate amount of Al$_2$O$_3$-CeO$_2$ support and Pt(NH$_3$)$_4$Cl$_2$. H$_2$O are put into the ethanol. Then, the reflux glass system is put on a stirrer. Solution is stirred continuously and temperature of the solution is stabled at around 80 °C which is boiling point of ethanol. The solution is refluxed for one day. After one day, most of the solution is still refluxed but some amount of ethanol is gone out of the system. It takes several hours to finish all ethanol and the remaining solid phase, which is Pt/Al$_2$O$_3$-CeO$_2$, in the glass, is taken. Figure 20 shows reflux system.
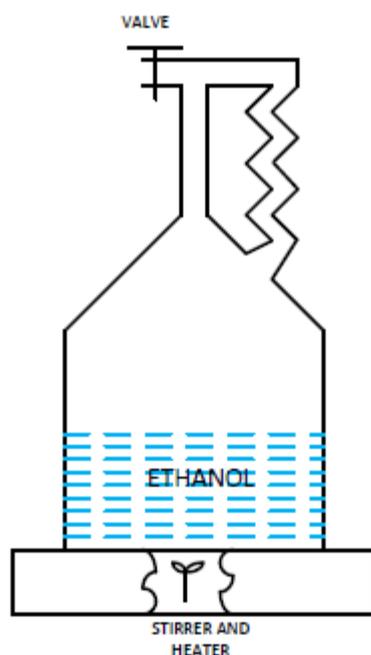
Figure 19. Reflux system

3.3 Experimental Setup

There are two different temperature programmed desorption (TPD) experimental setups. One of them is made by monitoring with thermal conductivity detector (TCD) and the other one with mass spectrometer (MS). In both systems, mass flow controllers (MFC) are used to be able to arrange flow amount in the system and mass flow controller station (MFCS) is used to be able to arrange MFCs. MFCs in the systems are Teledyne Hastings 200 series and MFCS is TRL Instrument MFCS. MS is Hiden HPR 20.

3.3.1 TPD System with TCD

There are two MFCs, one MFCS, one furnace, one temperature controller, three three way valves and one TCD in this system. This system has two different purposes. One of them is to desorb a molecule from sample and the other one is to adsorb CO_2 and H_2O to the material. Three way valves make these two different processes available with this one system. If one wants to make adsorption, gas which is wanted to adsorbed can be given directly to the sample. Figure 20 shows this experiment with the system.
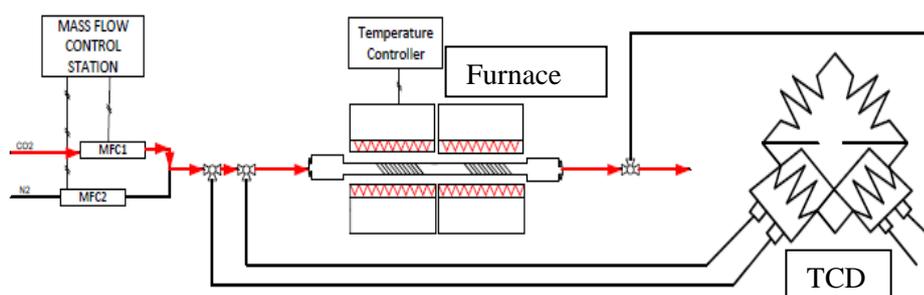
Figure 20. Adsorption experiment with TPD system with TCD

If one wants to make desorption, reference gas of TCD can be given directly to the reference cell of detector. After it goes out from the reference cell, it goes to inlet of furnace. Then, the reference gas with desorbed gas goes to sample cell of TCD. Figure 21 shows this experiment with the system.
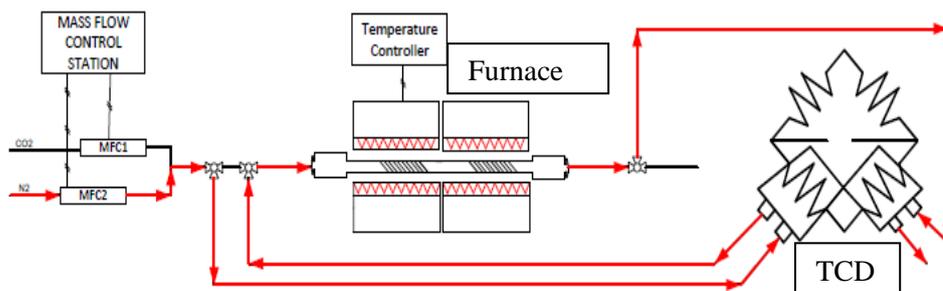
Figure 21. Desorption experiment with TPD system with TCD

The switch between the adsorption and desorption was carried out by manual operation of three way valves.

3.3.2 TPD System with MS

There are two MFCs, one MFCS, one furnace, one temperature controller, one three way valve and one MS in this system. System has two different purposes. One of them is desorbed a molecule from sample and the other one is giving a molecule to the sample to be adsorbed. Three way valve makes these two different processes available with this one system. If one wants to make adsorption, gas which is wanted to adsorbed can be given directly to the sample. If one wants to make desorption, other gas can be given directly to the furnace by changing the position of three way valve. Figure 22 and Figure 23 show these two different experiment pathways with the system.
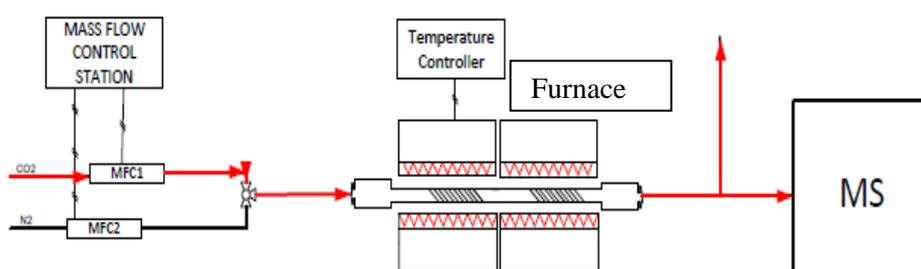
Figure 22. Adsorption experiment with TPD system with MS

30
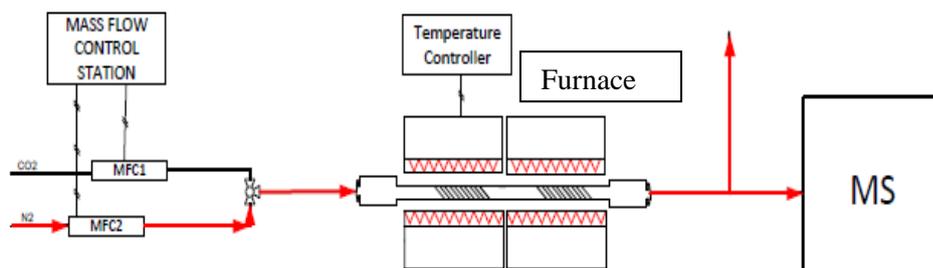
Figure 23. Desorption experiment with TPD system with MS

3.3.3 Dispersion Measurements

A chemisorption experiment system is used for making dispersion measurements. [74] There is a multi-way valve to select gas that is given into the system. There is one three way valve to choose the system that is wanted to use. VN1 and VV1 valves are used for adjusting inlet gas amount. VV5 valve is used for adjusting outlet gas amount. There is also a vacuum pump and a pressure sensor in the system. Drawing of the experimental system can be seen in figure 24.
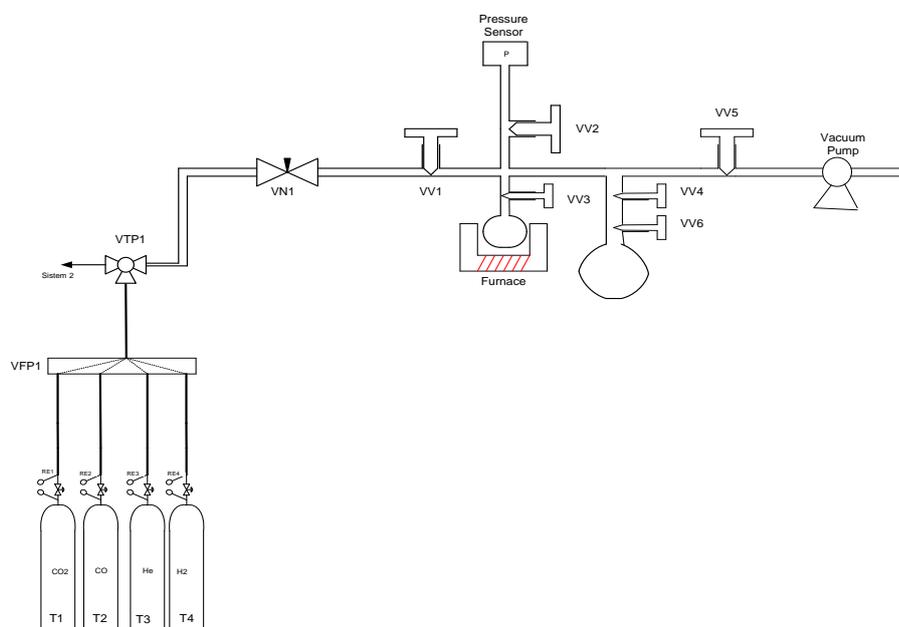
Figure 24. Drawing of chemisorption system used to measure metal dispersions

3.4 Experimental Procedures

In this study, CO_2 desorption, H_2O desorption and O_2 desorption experiments were performed. The detailed procedures of these experiments are given in Appendix F. Furthermore, the detailed protocol of dispersion measurements of the catalysts including the gas injection part, dispersion experiment part, dead volume measurement, reduction procedure, total adsorption and weak adsorption parts are also given in Appendix F.

CHAPTER 4

RESULTS AND DISCUSSION

In this part of thesis, TPD experiments with TCD and MS, dispersion experiments and surface area experiments results are given. These results are also discussed in this part. All TPD spectra are also given.

4.1 General TPD Analysis

TPD results of Pt/Al_2O_3-CeO_2, Al_2O_3-CeO_2 and Al_2O_3 are shown in Figure 25, Figure 26 and Figure 27 respectively. While Al_2O_3 sample is a commercial material, Al_2O_3-CeO_2 and Pt/Al_2O_3-CeO_2 samples are produced by incipient wetness method. TCD is used for gas monitoring for all experiments. Two different adsorption sites for Al_2O_3 and Al_2O_3-CeO_2 samples were deduced from the two separate peaks in the TPD diagrams. Pt/Al_2O_3-CeO_2 sample has three different adsorption sites identified by the peaks at 100, 340 and 650 °C. The desorbed materials cannot be identified from these experiments because a TCD was used. However, it can be said that Pt/Al_2O_3-CeO_2 has more desorption capacity in the same condition in comparison to other materials. Desorbed material amounts are calculated by calculating the area under the curves.and shown in Table 5. Desorbed material amount of Al_2O_3 is taken 1 and the others are normalized with respect to Al_2O_3. Although there is an oxygen peak for CeO_2-Al_2O_3 at about 400 ^{0}C in figure 15, this peak can not be seen in my experiments. The reason can be crystal structure difference of materials or detector sensitivity difference of detector.
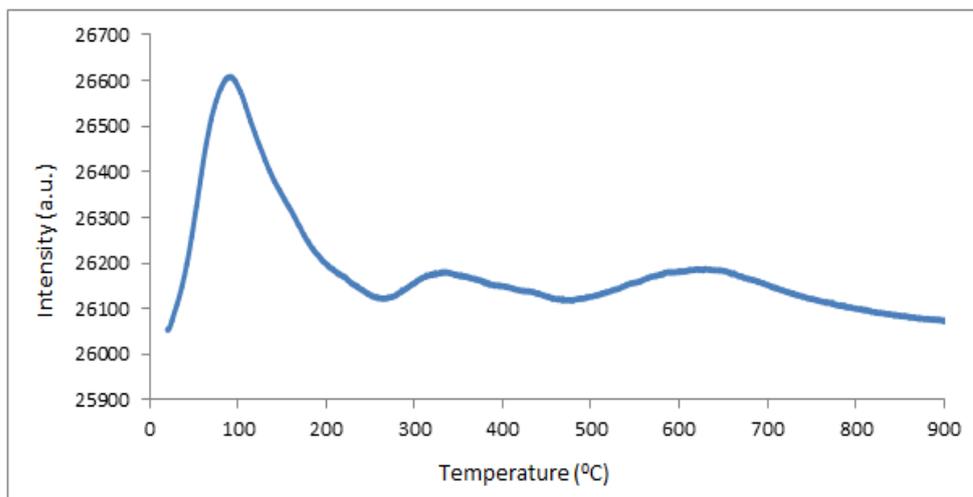
Figure 25. TPD graph of $Pt/Al_2O_3-CeO_2$; flow rate is 30 ml/min Nitrogen; heating rate $20^0C/min$.
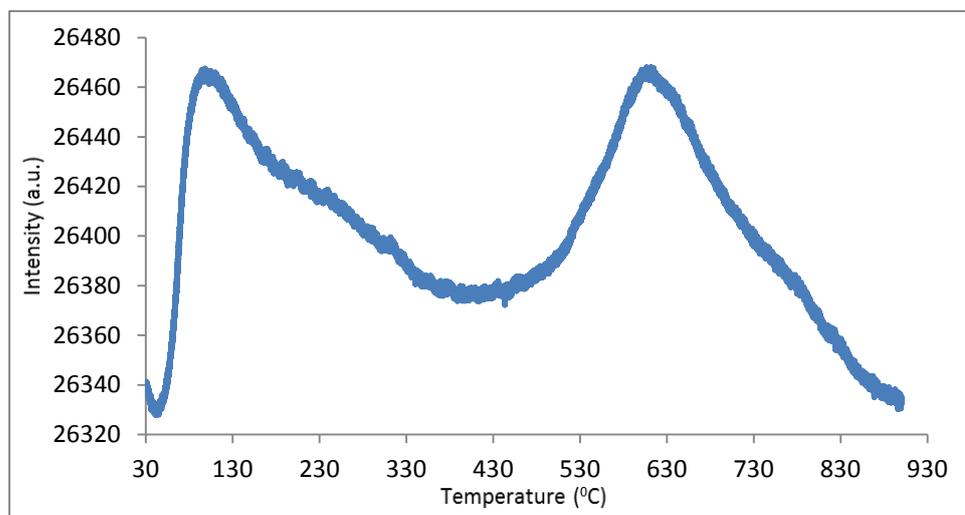
Figure 26. TPD graph of $Al_2O_3-CeO_2$; flow rate is 30 ml/min Nitrogen; heating rate $20^0C/min$
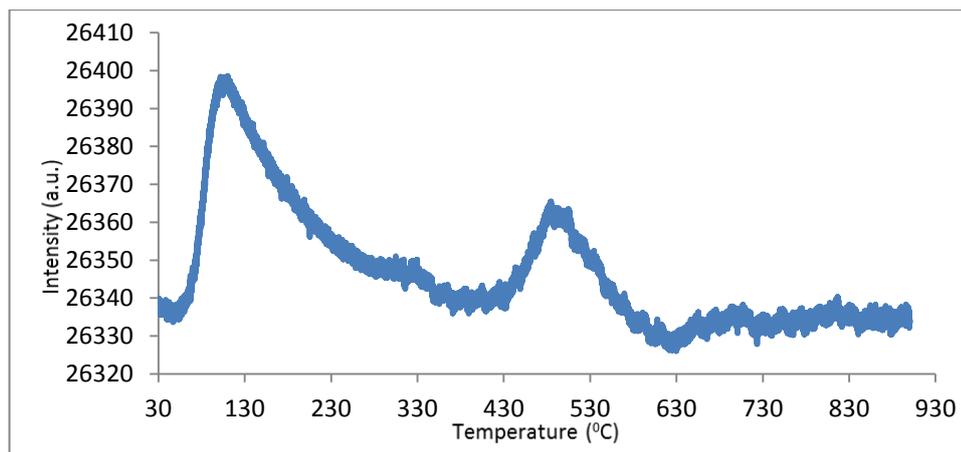
Figure 27. TPD graph of Al_2O_3; flow rate is 30 ml/min Nitrogen; heating rate 20^0C/min

Table 5. Desorption amounts normalized by the area of Al_2O_3, Al_2O_3-CeO_2 and Pt/Al_2O_3-CeO_2

Material	Desorption amount (Normalized by the area of Al_2O_3)
Al_2O_3	1
Al_2O_3-CeO_2	5.8
Pt/CeO_2	19

4.2 H_2O TPD Experiments

H_2O TPD experiments are made with Pt/Al_2O_3-CeO_2 sample with 0.5% Pt concentration and Pt/Al_2O_3-CeO_2 sample with 1% Pt concentration. Gas monitoring for these experiments was made by mass spectrometer. While monitoring, only 18 amu is monitored with MS. Figure 28 and Figure 29 show H_2O TPD spectra of samples. They show that there is only one peak in H_2O TPD spectra of Pt/Al_2O_3-CeO_2 sample. It means that H_2O molecules are made only one type of bond to the surface of the sample. According to asymmetric peak shapes in the spectra, desorption order of H_2O from sample can be found as first order desorption. Areas under the curves are also calculated by trapezoidal rule. The area amount of 1% Pt/Al_2O_3-CeO_2 is taken 1 and the result of the other one is calculated according to this assumption. Table 6 shows the sample which has 1% Pt concentration can adsorb higher amount of H_2O molecules.
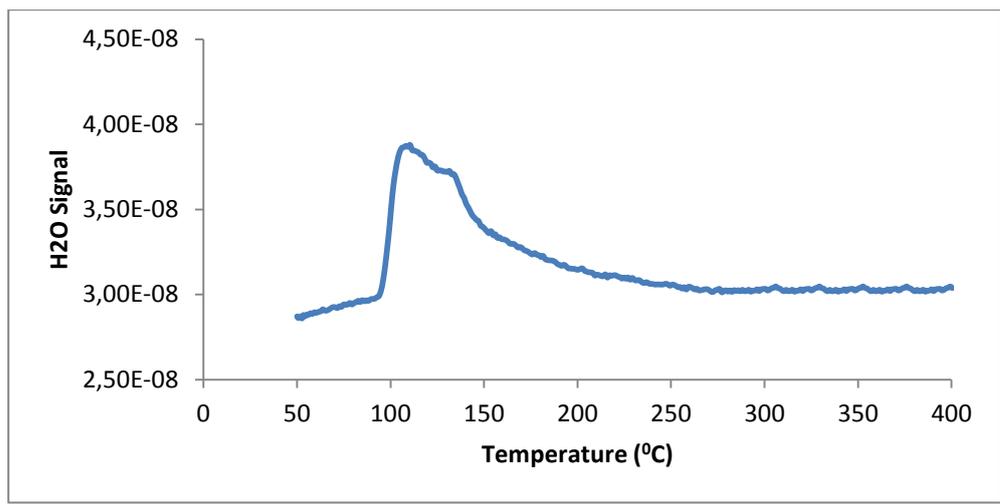
Figure 28. H_2O TPD spectrum of 0.5% Pt/Al_2O_3-CeO_2 ; flow rate is 30 ml/min Nitrogen; heating rate 20^0C/min
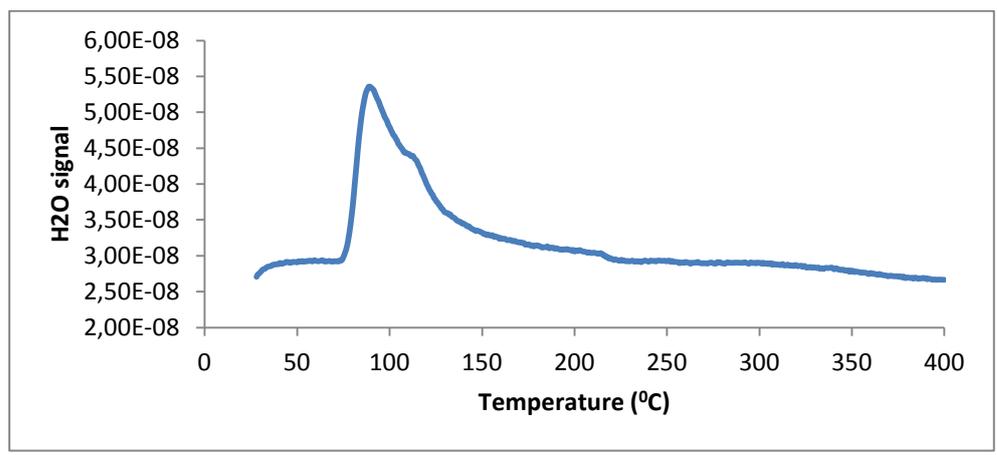
Figure 29. H_2O TPD spectrum of 1% Pt/Al_2O_3-CeO_2 ; flow rate is 30 ml/min Nitrogen; heating rate 20^0C/min

Table 6. H_2O desorption amount of 1% Pt/Al_2O_3-CeO_2 and 0.5% Pt/Al_2O_3-CeO_2

Material	Desorption Amount
1% Pt/Al_2O_3-CeO_2	1
0.5% Pt/Al_2O_3-CeO_2	0.63

4.3 CO_2 TPD Experiments

CO_2 TPD experiments are made for Pt/Al_2O_3-CeO_2 sample with 0.5% Pt concentration and Pt/Al_2O_3-CeO_2 sample with 1% Pt concentration. Gas monitoring for 44 AMU was made by a mass spectrometer. Figure 30 and Figure 31 show CO_2 TPD spectra of samples. They show that there is only one peak in CO_2 TPD spectra of Pt/Al_2O_3-CeO_2 sample. It means that CO_2 molecules only make one type of bond to the surface of the sample. According to nearly symmetric peak shapes in the spectra, desorption order of CO_2 from sample can be second order. Areas under the curves are also calculated by Trapezoidal Rule. The area amount of 1% Pt/Al_2O_3-CeO_2 is taken 1 and the result of the other catalyst is normalized with respect to this peak. Table 7 shows the sample which has 1% Pt concentration can adsorb much higher amount of CO_2 molecules, as anticipated.
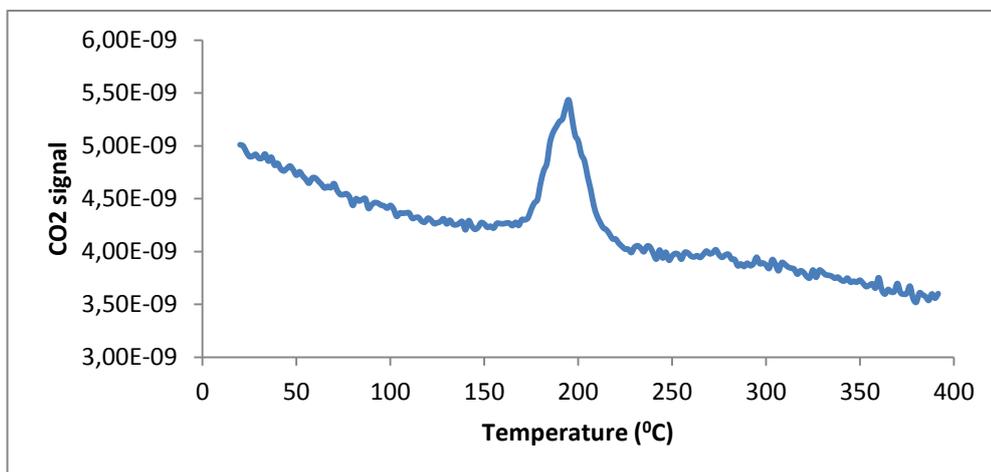
Figure 30. CO_2 TPD spectrum of 0.5% Pt/Al_2O_3-CeO_2 ; flow rate is 30 ml/min Nitrogen; heating rate 20^0C/min
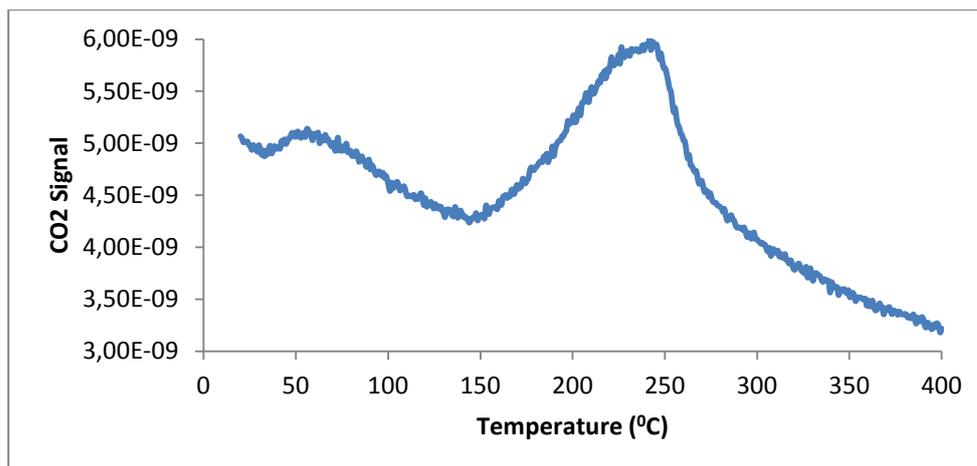
Figure 31. CO_2 TPD spectrum of 1% Pt/Al_2O_3-CeO_2 ; flow rate is 30 ml/min Nitrogen; heating rate $20^0C/min$

Table 7. CO_2 desorption amount from 1% Pt/Al_2O_3-CeO_2 and 0.5% Pt/Al_2O_3-CeO_2

Material	Desorption Amount
1% Pt/Al_2O_3-CeO_2	1
0.5% Pt/Al_2O_3-CeO_2	0.22

4.4 Flow Reversal System Design and O_2 TPD Experiments

O_2 TPD experiments are made over 1% Pt/CeO_2 and 1% Pt/Al_2O_3-CeO_2 catalysts. A flow reversal system was also designed to take oxygen from metal oxide and re-oxidize the reduced metal oxide automatically. Figure 32 shows piping and instrumentation diagram of the system.
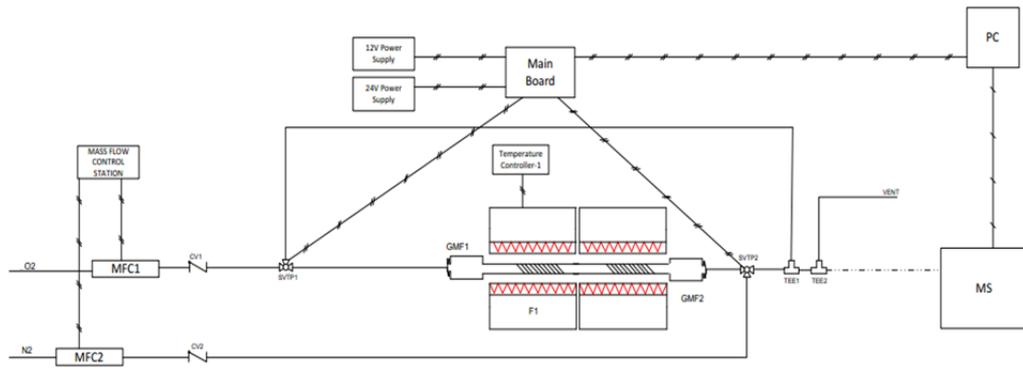
Figure 32. P&ID of the reversal system for reducing and oxidizing metal oxides

There are two three way valves (SVTP1 and SVTP2), an oven, two mass flow controllers (MFC1 and MFC2), a mass flow control station (MFCS), a PC and a mass spectrometer (MS) in the system. Three way valves are used to change gas flow direction and type of the gas. There are two semi cycles in an experiment. In one semi cycle, nitrogen is fed into system in one direction. On the other hand, carbon dioxide is fed into system in opposite direction in the other semi cycle. These two three way valves can be controlled with an electronic board by an interface program from PC. The heating fort he reactor is provided by a furnace. Equipped with a temperature controller (Honeywell DC 1010). Teledyne Hastings 200 series mass flow controllers are used to adjust the flow rate of the gases. MFCs monitoring and control are achieved by a Terralab Instrument MFCS. A portion of the outlet gas is taken into Hiden HPR 20 mass spectrometer for analysis. Rest of the outlet gas is purged to vent. Figure 33 and Figure 34 show the pathways of two different semi cycles of the system.
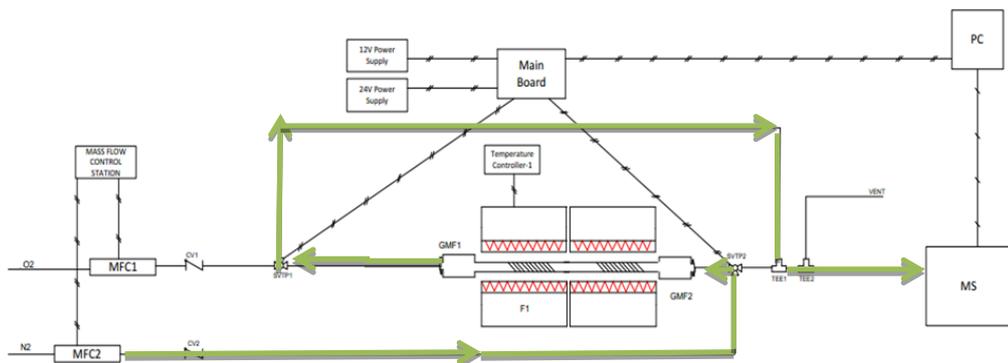
Figure 33. Oxygen desorption semi cycle of RFR system
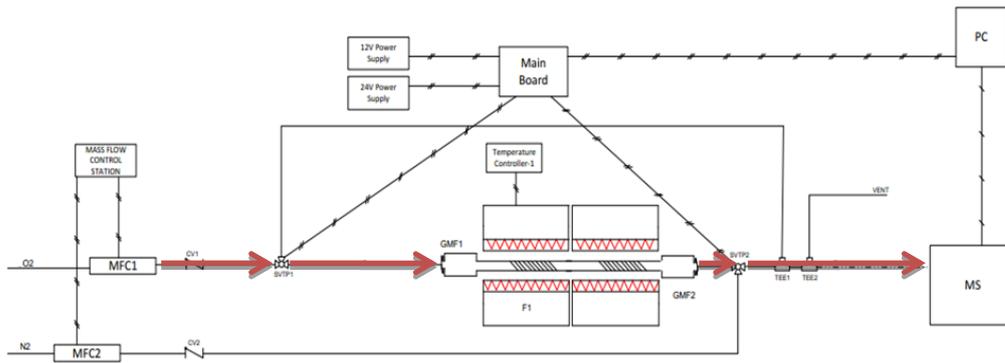
Figure 34. Re-oxidation semi cycle of RFR system

Automation of the system is provided by an electronic board and a simple software which can arrange the position and timing of the three way valves. The software is custom written by a software engineer from Terralab. Codes could be found in Appendix A. The board originally designed for a Trl-TOC instrument by Terralab found to be also convenient for RFR system. Figure 35 shows the picture of the board.

Figure 35. Picture of the board

O$_2$ TPD spectrum of Pt/CeO$_2$ shows that there is only oxygen desorption at about 700 ^{0}C; however, spectrum of Pt/Al$_2$O$_3$-CeO$_2$ shows that there are two oxygen desorption peaks at about 700 and 950 ^{0}C. These two spectra give information about oxygen desorption from bulk is possible for Pt/Al$_2$O$_3$-CeO$_2$ catalyst. Figure 36 and Figure 37 show O$_2$ TPD spectra of Pt/CeO$_2$ and Pt/Al$_2$O$_3$-CeO$_2$.
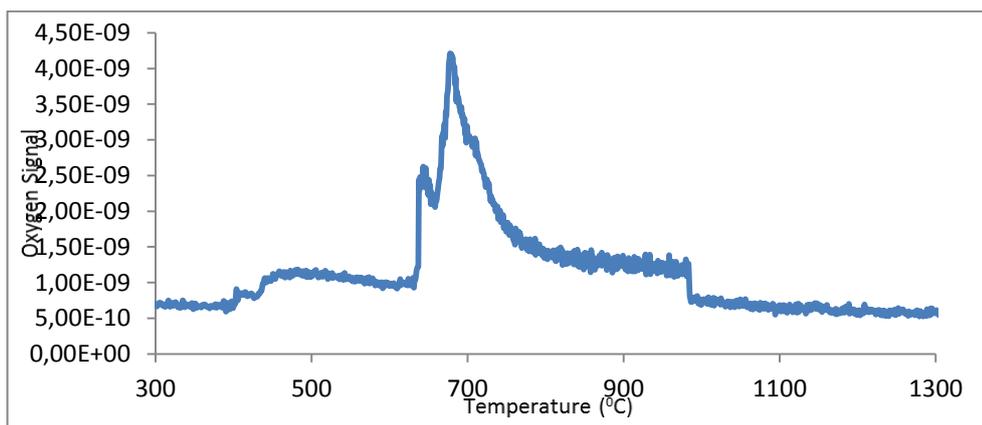
Figure 36. O$_2$ TPD spectrum of Pt/CeO$_2$; flow rate is 30 ml/min Nitrogen; heating rate 20^{0}C/min
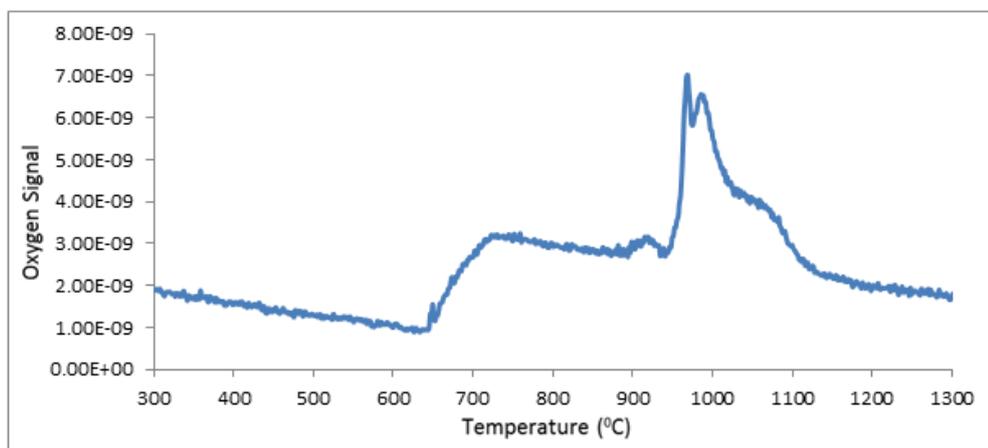
Figure 37. O$_2$ TPD spectrum of Pt/Al$_2$O$_3$-CeO$_2$; flow rate is 30 ml/min Nitrogen; heating rate 20^{0}C/min

A series of experiments were also done to demonstrate the operation of flow reversal system. O_2 TPD spectrum for 5 consecutive cycles is shown in figure 38. System can desorb oxygen and oxidize again. In the first cycle, nitrogen gas was sent to reactor. After the desorption data was collected, the system was cooled under nitrogen flow, and then CO_2 passed through the reactor for reoxidation. This procedure was done for all cycles. Table 8 shows oxygen desorption amount of all cycles. Oxygen desorption amount calculations were determined after calibration of the MS signal against injections of 100μL, 250μL and 500μL oxygen into the empty system. Areas of the peaks of these oxygen injections were calculated and a calibration equation was created from these data. Area and calibration equation data are in appendix E.
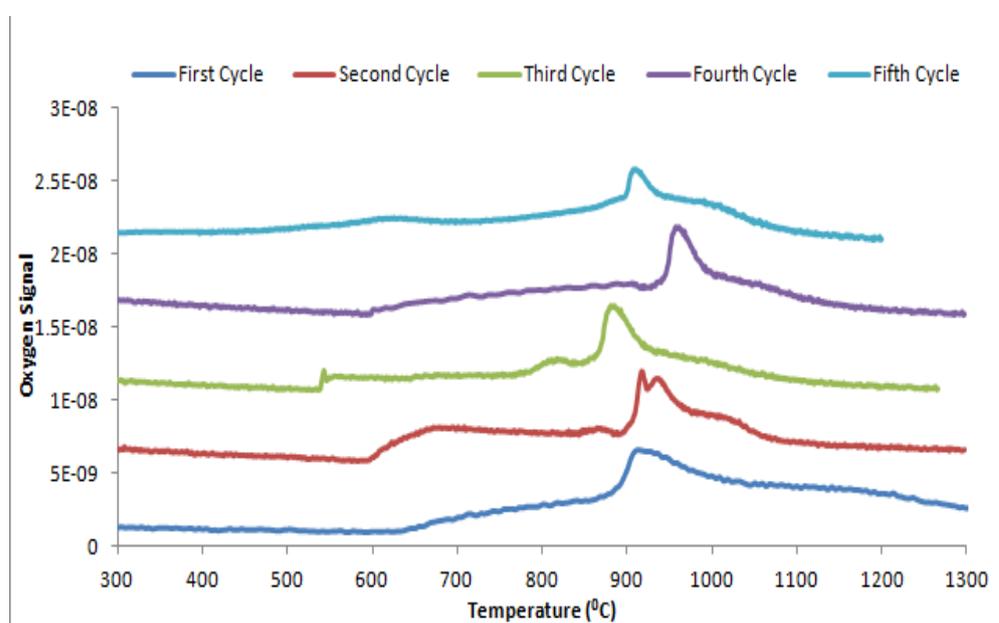
Figure 38. O_2 TPD spectrum of Pt/Al$_2$O$_3$-CeO$_2$ for 5 consecutive cycles; flow rate is 30 ml/min Nitrogen; heating rate 20^{0}C/min

After the sample is oxidised by CO_2, oxygen can be desorbed from sample. By this way, it can be understood that CO_2 is reduced while the sample is oxidised. However, it is very hard to see CO signal with MS due to CO_2 also gives signal at 28 amu. One additional experiment is also done to see CO signal because of CO_2 reduction. To this purpose 0.1 ml CO_2 is given into 30 ml/min He flow at 300^{0}C after oxygen desorption of Pt/Al$_2$O$_3$-CeO$_2$. By this way, all the CO_2 molecules are reduced and CO molecules can be seen with MS (Figure 39).

Table 8. Oxygen desorption amount of for 5 consecutive cycles

Number of Cycle	Oxygen Desorption (μmole)	Desorbed oxy./Total oxy. (%)
1	3.15	6.97
2	0.9	1.98
3	0.93	2.05
4	1.03	2.26
5	0.86	1.9
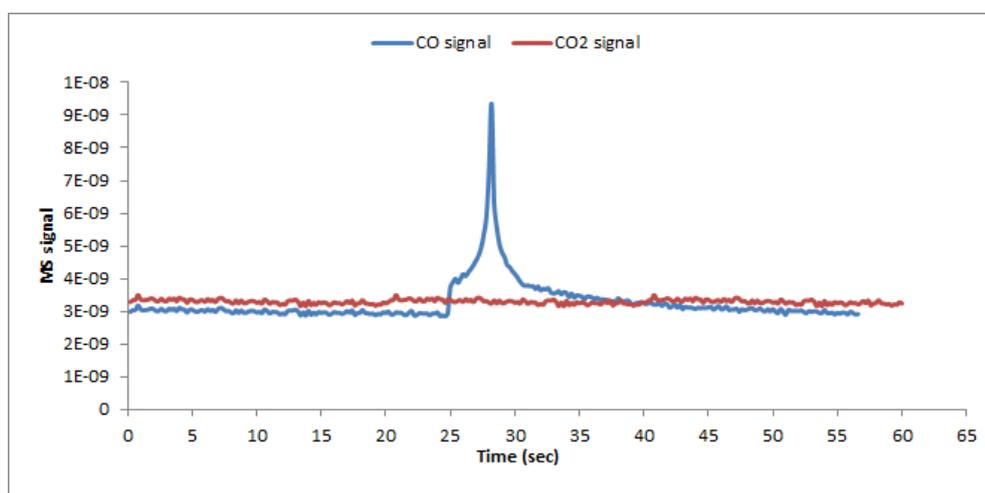
Figure 39. CO signal from CO_2 reduction; flow rate is 30 ml/min Helium; temperature is 300^0C

4.5 Pt Effect on O_2 Desorption from CeO_2

Effect of Pt on O_2 desorption amount from CeO_2 was also investigated in this work. First, the phase diagram of ceria (Figure 40) was used to find out the resulting compound after O_2 desorption. Then, equilibrium conversion (X_e) was determined for $2CeO_2 \rightarrow Ce_2O_x + (4-x)/2$ O_2 reaction as a function of temperature.
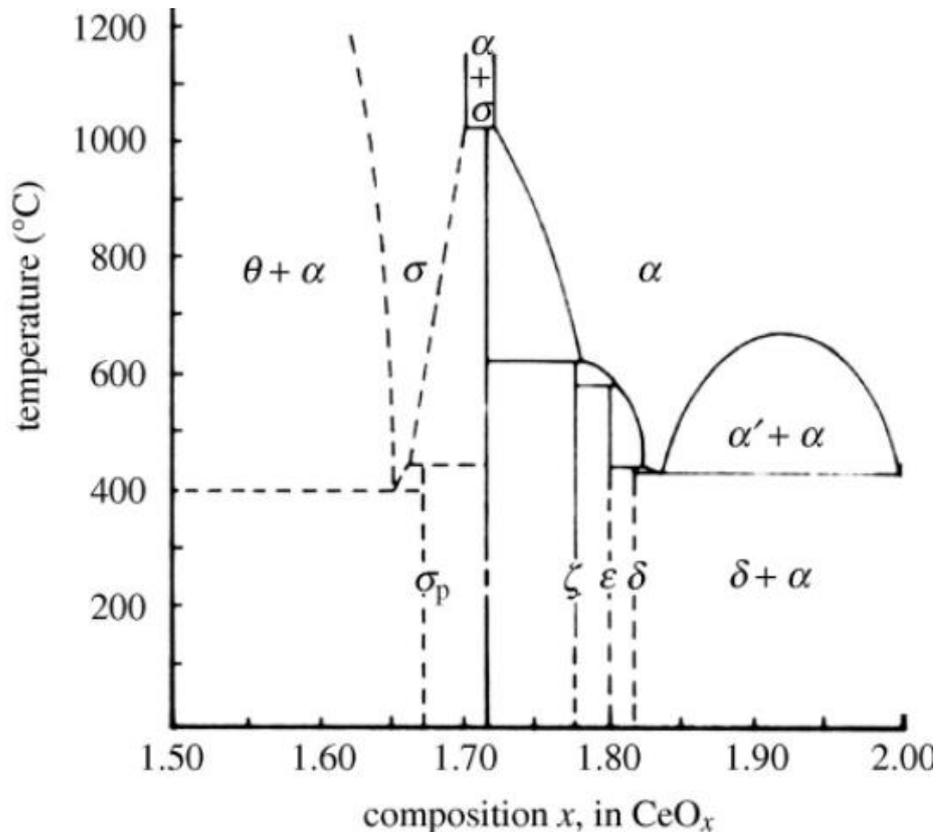
Figure 40. Phase diagram of ceria [75]

Predominance diagram of ceria as a function of oxygen pressure was also drawn to show that CeO_2 can go to Ce_2O_3 form only. Stability of ceria can be determined by the formation equilibrium constant of reactions. Calculations for predominance diagram can be found in Appendix B. Figure 41 shows predominance diagram of ceria as a function of oxygen partial pressure. Diagram shows that direct reduction of CeO_2 to Ce is not possible.
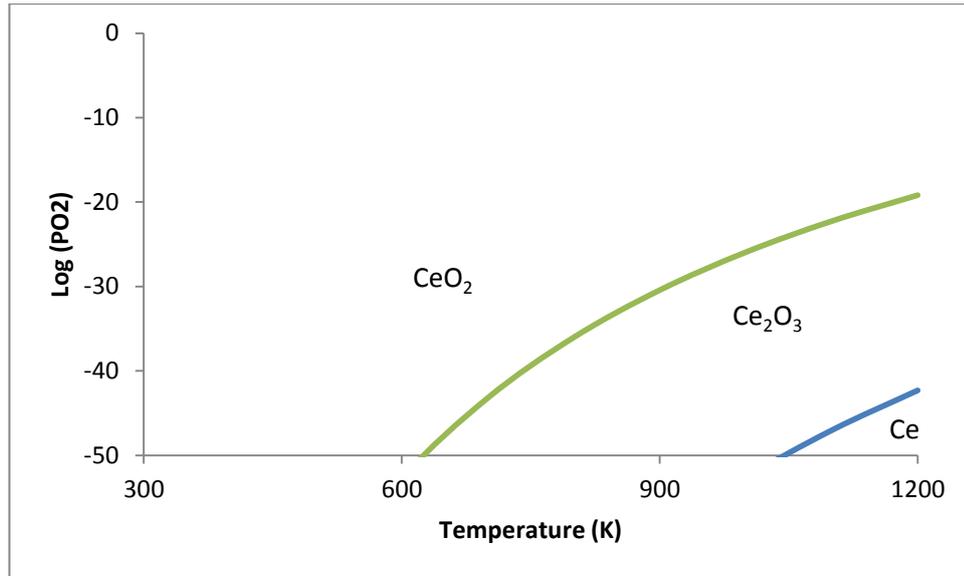
Figure 41. Predominance diagram of ceria according to oxygen atmosphere

It is seen that CeO_2 can be turned into Ce_2O_3 form after O_2 desorption from phase diagram. It cannot be turned into pure Ce form. So, the reaction of O_2 desorption of CeO_2 is;

$$2CeO_2 \leftrightarrow Ce_2O_3 + {}^1\!/_2\, O_2 \qquad (4.1)$$

The equilibrium conversion calculations for equation (4.1) were made and X_e vs temperature graph was drawn. Equilibrium conversion calculation can be seen in Appendix B. Figure 42 and Figure 43 show X_e vs temperature graphs of pure ceria. Since Ce_2O_3 to Ce reaction does not happen, it is not included in the calculations.
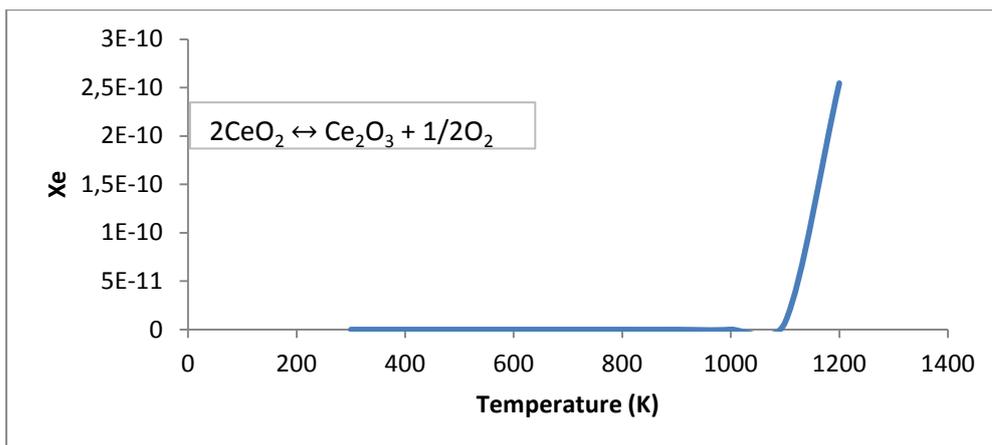
Figure 42. Equilibrium vs temperature graph of pure CeO_2 at low temperatures
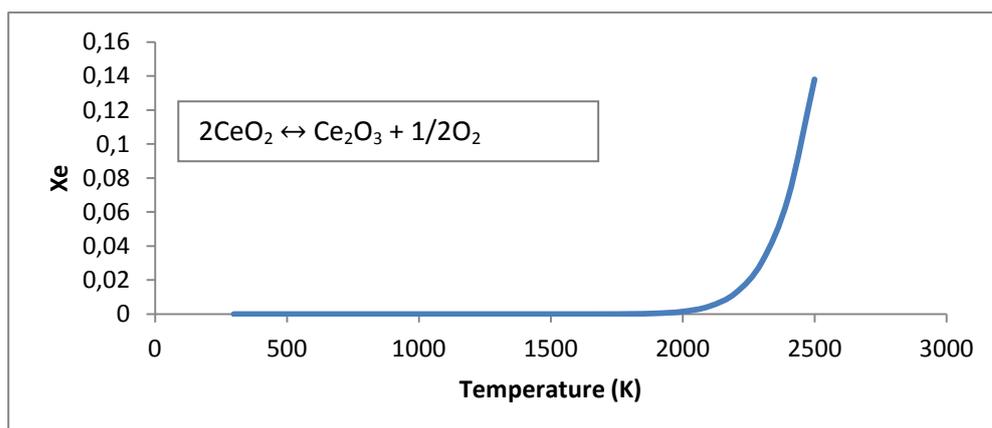
Figure 43. Equilibrium vs temperature graph of pure CeO_2 at high temperatures

It can be seen that conversion of O_2 desorption increases significantly after 2000 K. Before this temperature, conversion amount is nearly zero. O_2 TPD experiment with Al_2O_3-CeO_2 was also done after these calculations. Oxygen monitoring was made by MS in this experiment. Figure 44 shows the result of O_2 TPD experiment with Al_2O_3-CeO_2.
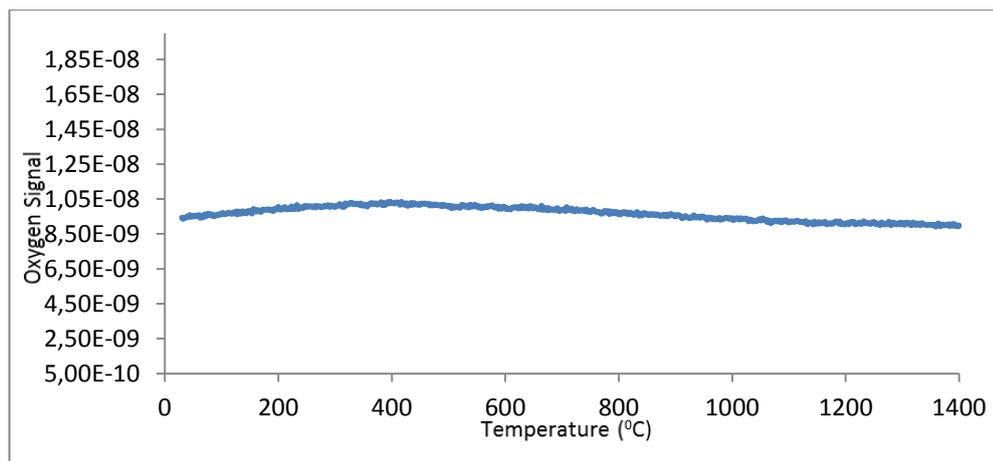
Figure 44. O_2 TPD spectrum of Al_2O_3-CeO_2 ; flow rate is 30 ml/min Nitrogen; heating rate 20^0C/min

O_2 TPD experiment with pure CeO_2 shows that there is no oxygen signal until 1400^0C. However, one can see oxygen desorption peak in figure 37 which shows O_2 TPD spectrum of 1% Pt/Al_2O_3-CeO_2. These two TPD spectra and equilibrium conversion calculation results show that Pt can lower O_2 desorption temperature.

4.6 O_2 TPD comparison of the Catalysts Prepared by Polyol Method and and Incipient Wetness Method

In this work, two different catalyst preparation methods were used the incipient wetness and the polyol method. 1wt % Pt/Al_2O_3 catalyst was prepared with both methods. This experiment was made by O_2 desorption experiment procedure at Appendix F. Figure 45 shows the O_2 TPD spectra of the two catalysts. O_2 desorption amount of the catalysts was calculated by calculating the area under the curves. Trapezoidal rule was used to calculate area. Then, this calculated area is put into calibration equation that is made by signal of known oxygen amounts. Number of moles of desorbed oxygen can be found by this way. Percentage of desorbed oxygen amount per total oxygen amount in catalyst is also calculated. Table 9 shows results for these catalysts.
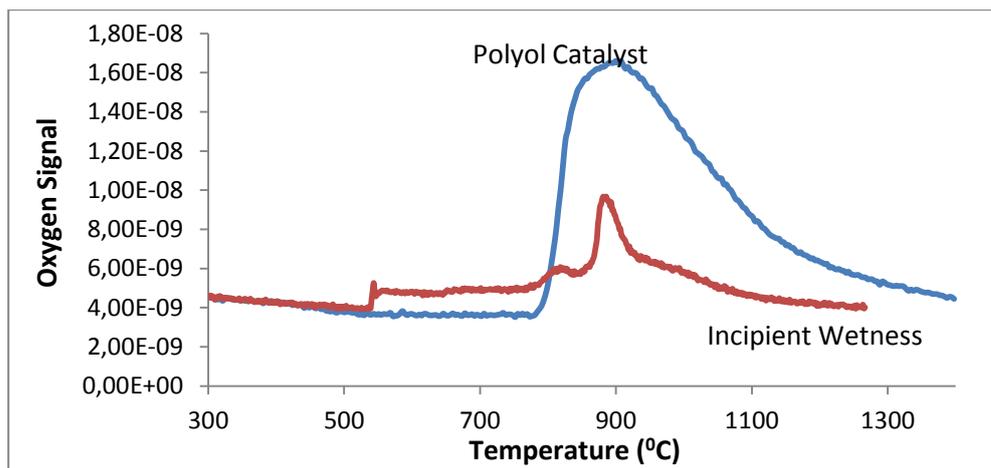
Figure 45. O_2 TPD spectra of incipient wetness and polyol catalysts; flow rate is 30 ml/min Nitrogen; heating rate $20^0C/min$

Table 9. O_2 desorption amount, dispersion results and surface area results of 1% Pt/Al_2O_3-CeO_2 incipient wetness and 1% Pt/Al_2O_3-CeO_2 polyol

Preparation Method	Oxygen Desorption (μmole)	Desorbed oxy./Total oxy. (%)	Metal dispersion (%)	Surface area (m^2)
Polyol	5.26	9.95	24.2	62.1
Incipient Wetness	0.93	1.76	52.9	67.4

Dispersion calculations and experimental data are in Appendix D section. Surface areas of these catalysts are also investigated. This characterization is made by N_2 adsorption method by Micromeritics tristar II 3020 equipment. There is no big difference between surface areas of the catalysts as it is expected because they have same support.

There is also a color difference between CeO_2 and Ce_2O_3. CeO_2 has pale yellow color whereas Ce_2O_3 has a color between green and grey. Ce_2O_3 is not a stable crystal form. If it touches to any oxygen source, it turns to CeO_2 suddenly and getting pale yellow color again. Because of this reason, there is no chance of investigating Ce_2O_3 with XRD or Raman Spectroscopy without in situ methods.
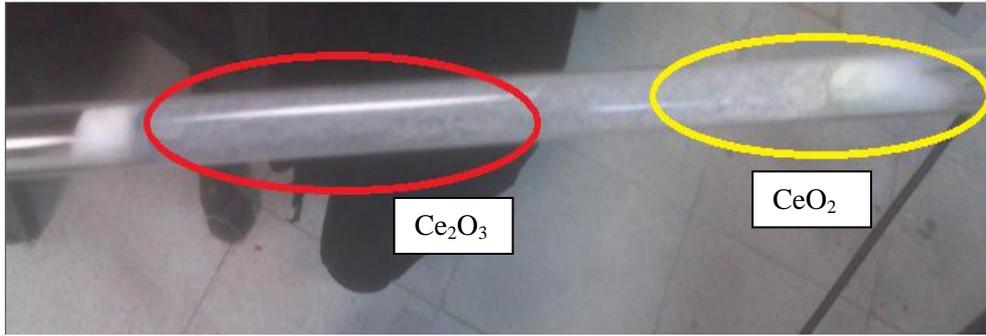
Figure 46. Color difference between CeO_2 and Ce_2O_3

CHAPTER 5

SUMMARY AND CONCLUSIONS

In the scope of this thesis, two different TPD systems were constructed. One of them is made detection with TCD and the other one is detected with MS. Pt/Al_2O_3-CeO_2 showed higher adsorption and desorption capability than Al_2O_3 and Al_2O_3-CeO_2 by general TPD analysis. H_2O TPD experiments showed that catalyst with higher amount of Pt has higher H_2O adsorption capability. Experiments also showed that H_2O desorption from Pt/Al_2O_3-CeO_2 is first order desorption. CO_2 desorption experiments are also done. These experiments showed higher Pt concentration enhances CO_2 adsorption drastically. However, this time desorption was second order desorption. Effect of Pt on oxygen desorption temperature was investigated. It is shown that Pt can lower oxygen desorption temperature from CeO_2.

An automatic flow reversal system was also designed and constructed to be able to make cyclic reduction and oxidation reactions with metal oxide. O_2 desorption and metal oxidation reactions were made this system. Results showed that system works properly. Experiments also showed O_2 desorption from Pt/Al_2O_3-CeO_2 is higher than O_2 desorption from Pt/CeO_2. Comparison of oxygen desorption amount between the catalysts which was produced by reflux method and incipient wetness method was made. Catalyst made by reflux method gave higher oxygen desorption amount.

REFERENCE

[1]   Symposium on Cyclic Processing Operations, Ind. Eng. Chem., Proc. Des. Dev., 6 (1967), 2 – 48

[2]   F. J. M. Horn, and R. C. Lin, Ind. Eng. Chem., Proc. Des. Dev., 6 (1967), 21

[3]   J. M. Douglas, and D. W. T. Rippin, Chem. Eng. Sci., 21 (1966), 305

[4]   J. E. Bailey, and F. J. M. Horn, Ber. Bunsenges Phys. Chem., 73 (1969), 274

[5]   G. K. Boreskov, and Yu. Sh. Matros, Catal. Rev. Sci. Eng., 25 (1984), 551

[6]   G. K. Boreskov, G. A. Bunimovich, Yu. Sh. Matros, and A. A. Ivanov, Kinet. Catal., 23(1982), 402

[7]   M. Luther, J. J. Brandner, L. Kiwi-Minsker, A. Renken, and K. Schubert, Inter. Jour. of Chem. Reac. Eng., 5(2007), A49

[8]   P. Forzatti, and L. Lietti, Catalysis Today, 52 (1999), 165 – 181

[9]   C. Bartholomew, Applied Catalysis, A212 (2001), 17 – 60

[10]   A. K. Neyestanaki, F. Klingstedt, T. Salmi, and D. Y. Murzin, Fuel, 83 (2004), 395 – 408

[11]   A. Mitri, D. Neumann, T. Liu, and G. Veser, Chem. Eng. Sci., 59 (2004), 5527 – 5534

[12]   Y. S. Matros, Penn Well Books, 1994, 44 – 53

[13]   Y. S. Matros, Catalytic Processes under Unsteady State Conditions, Elsevier, Amsterdam, 1989

[14]   G. K. Boreskov, Y. S. Matros, V. I. Lugovskoy, G. A. Bunimovich, and V. I. Puzhilova, Teor. Osn. Khim. Technol., 18 (1984), 328

[15]   Y. S. Matros, A. S. Noskov, and V. A. Chumachenko, Chem. Eng. Processing, 32 (1993), 89

[16]   Y. S. Matros, G. A. Bunimovich, and G. K. Boresov, in Frontiers in Chemical Reaction Engineering, Vol 2 (L. K. Doraiswami, and R. A. Mashelkar, eds.), Wiley Eastern, New Delhi, 1984

[17]   Y. S. Matros, and G. A. Bunimovich, in Sulphur 1990, Cancun, Mexico, April 1 – 4, 1990 (British Sulphur Corporation Ltd, eds.), Gosport, Hants, 1990, 249

[18]   L. N. Bobrova, E. M. Slavinskaya, A. S. Noskov, and Y. S. Matros, React. Kinet. Catal. Lett., 37 (1988), 267

[19]   A.S. Noskov, L. M. Bobrova, and Y. S. Matros, Catal. Today, 17 (1993), 293

[20]   M. Sheintuch and O. Nekhamkina, Chemical Engineers AICHE J, 51 (2005), 224 – 234

[21]   Michigan State University, CEM 924 notes, Spring 2001

[22]   J. Happel, Journal of Chem. Eng. Sci., 33 (1978), 1567

[23]   C.O. Bennett, ACS Symposium Series Washington, 178 (1982), 1

[24]   P.J. Biloen, J. Mol. Cat., 21 (1983), 17

[25]   C. Breitkopf, Leipzig University (Modern Methods in Heterogeneous Catalysis), 2003

[26]   J. L. G. Fierro, CRC Press, Metal Oxiddes, 2005, 217

[27]   P. Mars and D. W. van Krevelen, Chem. Eng. Sci., 3 (1954), 41 – 59

[28]   A. Bielanski and J. Haber, Oxygen in Catalysis; Chemical Industries Series; Marcel Dekker: New York, 1991; Vol. 43, pp. 1–448.

[29]   J. Haber, and B. Grzybowska, J. Catal., 28 (1973), 489–505.

[30]   B. Grzybowska, J. Haber, and J. Janas, J. Catal., 49 (1977), 150–163.

[31]   R. K. Grasselli, and J. D. Burrington, Adv. Catal., 30 (1981), 133–163.

[32]   R. K. Grasselli, Top. Catal., 15 (2001), 93–101.

[33]   J. C. Védrine, J. M. M. Millet, and J. C. Volta, Catal. Today, 32 (1996), 115–123.

[34]   J. C. Védrine, G. Coudurier, and J. M. M. Millet, Catal. Today, 33 (1997), 3–13.

[35]   S. Bernal, J. Kasper, and A. Trovarelli, Catal. Today, 50 (1999), 173–443.

[36]   A. Trovarelli, Catalysis by Ceria and Related Materials; Catalytic Science Series; World Scientific Publishing Company: U.K., 2002; Vol. 2, 1–309.

[37]   A. Trovarelli, C. de Leitenburg, and G. Dolcetti, Chemtech, 27 (1997), 32–37.

[38]   K. C. Taylor, Catalysis Science and Technology; Springer-Verlag: Berlin, 1984; chapter 2.

[39]   A. Tschope, W. Liu, M. F. Stephanopoulos, and J. Y. Ying, J. Catal., 157 (1995), 42–50.

[40]   B. T. Kilbourn, Cerium, a Guide to its role in Chemical Technology; Molycorp Inc.: White Plains, NY, 1992.

[41]   H. S. Gandhi, G. W. Graham, and W. W. McCabe, J. Catal., 216 (2003), 433–442

[42]   S. S. Lin, C. L. Chen, D. J. Chang, and C. C. Chen, Water Research, 36 (2002), 3009 – 3014.

[43]   I. P. Chen, S. S. Lin, C. H. Wang, L. Chang, J. S. Chang, App. Cat. B: Environmental, 50 (2004), 49 – 58

[44]   S. Sharma, S. Hilaire, J. M. Vohs, R. J. Gorte, and H.-W. Jeny, Jour. of Catal., 190 (2000), 199 – 204

[45]   Chueh, W.C. m, C. Falter, M. Abbott, D. Scipio, P. Furler, S. M. Haile, and A. Steinfeld, Science, 330 (2010), 1797

[46]   F. Gaillard, Catalysis Letters, 95 (2004), 1 – 2

[47]   D. Uner, and U. Oran, Applied Catalysis B: Environmental, 54 (2004), 183 – 191

[48]   Redhead, P. A., Thermal desorption of gases, Vacuum 12 (1962) 203-201.

[49]   Amenomiya, Y., Cvetanovic, R. J., Application of flash-desorption method to catalyst studies. III. Propylene alumina system and surface heterogeneity, J. Phys. Chem. 67 (1963) 2705-2708.

[50]   Falconer, J. L., Schwarz, J. A ., Temperature-programmed desorption and reaction: applications to supported catalysts, Catal. Rev.. Sci. Eng. 25 (1983) 141-227.

[51]   Lemaitre, J.L., Temperature-programmed methods, In Characterization of Heterogeneous Catalysts, Ed. Delannay, F., Marcel Dekker, Inc., New York 1984, pp. 29-70.

[52]   Tovbin, Y., Theory of adsorption.desorption kinetics on flat heterogeneous surfaces, In Equilibria and Dynamics of Adsorption on Heterogeneous Solid Surfaces, Eds. Rudzinski, W., Steele, W. A., Zgrablich, G., Vol. 104 of Stud. Surf. Sci. Catal., Elsevier, New York 1997, pp. 201-284.

[53]   Gorte, R. J., Temperature-programmed desorption for the characterisation of oxide catalysts, Catal. Today 28 (1996) 405-414.

[54]   Arena, F., A characterization study of the surface acidity of solid catalysts by temperature programmed methods, Applied Catalysis A: General 170 (1998) 127 - 137

[55]   Falconer, J.L., Madix, R.J., Desorption rate isotherms in flash desorption analysis, J. Catal. 48 (1977) 262-268.

[56]   Rudzinski, W., Borowiecki, T., Panczyk, T., Dominko, A., On the applicability of Arrhenius plot methods to determine surface energetic heterogeneity of adsorbents and catalysts surfaces from experimental TPD spectra, Adv. Colloid Interface Sci. 84 (2000) 1-26.

[57]   Russell, N. M., Ekerdt, J. G., Nonlinear parameter estimation technique for kinetic analysis of thermal desorption data, Surf. Sci. 364 (1996) 199-218.

[58]   Herz, R. K., Kiela, J. B., Marin, S. P., Adsorption effects during temperatureprogrammed desorption of carbon monoxide from supported platinum, J. Catal. 73 (1982) 66-75.

[59]   Rieck, J. S., Bell, A. T., Influence of adsorption and mass transfer effects on temperature-programmed desorption from porous catalysts, J. Catal. 85 (1984) 143 - 153.

[60]   Demmin R. A. Gorte, R. J., Design parameters for temperature-programmed desorption from a packed bed, J. Catal. 90 (1984) 32-39.

[61]   Ibok, E. E., Ollis, D. F., Temperature-programmed desorption from porous catalysts: shape index analysis, J. Catal. 66 (1980) 391-400.

[62]   Jansen A. P. J., Monte carlo study of temperature programmed desorption spectra with attractive lateral interactions, Physical Review B, 52 (1995) 7.

[63]   Wang, C. C. Et al., Microkinetic simulation of temperature programmed desorption, Journal of Physical Chemistry, 117 (2013) 6136 – 6142.

[64]   Fadoni M. and Lucarelli L., Temperature programmed desorption, reduction, oxidation and flow chemisorption for the characterisation of heterogeneous catalysts. Theoretical aspects, instrumentation and applications.

[65]   Miyazaki E., Chemisorption of Diatomic-Molecules (H-2, N-2, CO) on Transition D-Metals, 65 (1980) 84.

[66]   Iwamoto M. et al., Study of Metal Oxide Catalysts by Temperature Programmed Desorption.
1. Chemisorption of Oxygen on Nickel Oxide, Journal of Physical Chemistry, 80 (1976) 18

[67]   Iwamoto M. et al., Temperature-programmed Desorption Spectra of Oxygen from Transition Metal Ion-exchanged Y -Type Zeolites, J. C. S. Chem. Comm., (1976)

[68]   Iwamoto M. et al., Study of Metal Oxide Catalysts by Temperature Programmed Desorption. 4. Oxygen Adsorption on Various Metal Oxides, Journal of Physical Chemistry, 82 (1978) 24

[69]   Haegal S. et al., A technique for extending the precision and the range of temperature programmed desorption toward extremely low coverages, Review of Scientific Instruments, 81 (2010) 033904

[70]   Choi J. G. Et al., Temperature programmed desorption of H_2 from molybdenum nitride thin films, Applied Surface Science, 78 (1994) 299 – 307

[71]   Pirolli L. And Teplyakov A. V., Complex thermal chemistry of vinyltrimethylsilane on Si(100)-2 x 1, Journal of Physical Chemistry B, 109 (2005) 8462 – 8468

[72]   Guenard R. L. Et al., Selective surface reactions of single crystal metal carbides: alkene production from short chain alcohols on titanium carbide and vanadium carbide, Surface Science, 515 (2002) 103 - 116

[73]   Artsyukhovich A.N. et al., Low temperature sticking and desorption dynamics of oxygen on Pt(111), Surface Science, 347 (1996) 303 – 318

[74] Tapan, N.A. (1999). Adsorption dynamics and reaction kinetics at gas-solid interfaces: applications in catalysis and gas sensors. MSc. Thesis. Middle East Technical University. Turkey

[75]   A thermochemical study of ceria: exploiting an old material for new modes of energy conversion and CO2mitigation

A. SOFTWARE CODE FOR RFR SYSTEM

```csharp
using System;
using System.Collections.Generic;
using System.ComponentModel;
using System.Data;
using System.Drawing;
using System.Linq;
using System.Text;
using System.Windows.Forms;
//using DevExpress.XtraEditors;
using System.IO.Ports;
using System.Threading;

namespace WindowsFormsApplication1
{
    public partial class Form1 : Form
    {
        #region Degiskenler

        private int zaman;
        private int dak;
        private int sn;
        public bool veriGeldi = false;
        public enum MessageType { Incoming, Outgoing, Normal, Warning, Error
};
        public Color[] MessageColor = { Color.Blue, Color.Green, Color.Black,
Color.Orange, Color.Red };
        private string[] role_durumlar = new string[2] { "OFF", "OFF" };

        #endregion Degiskenler

        public Form1()
        {
            InitializeComponent();
        }

        #region RICHTEXTBOXLARA YAZDIR
        [STAThread]
        public void ekrandaGoster(MessageType type, string msg)
        {
            if (rtb1 != null)
            {

                rtb1.Invoke(new EventHandler(delegate
                {
                    rtb1.SelectedText = string.Empty;
                    rtb1.SelectionFont     =     new     Font(rtb1.SelectionFont,
FontStyle.Bold);
```

```csharp
                    rtb1.SelectionColor = MessageColor[(int)type];
                    rtb1.AppendText(msg);
                    rtb1.ScrollToCaret();
                }));
            }
            else
            {
                MessageBox.Show("Check Communication Settings");
            }
        }
        #endregion RICHTEXTBOXLARA YAZDIR

        #region MySerialPort Get/Set

        public SerialPort MySerialPort
        {
            get { return serialPort1; }
            set { serialPort1 = value; }
        }

        #endregion get/Set Functions

        #region PORT AÇ
        public bool portAc(string gelen)
        {
            try
            {
                    serialPort1.DataReceived += serialPort_DataReceived;
                    ekrandaGoster(MessageType.Normal,   "Port   is   open."   +
DateTime.Now + "\n");
                    serialPort1.Open();
                    return true;
            }
            catch (Exception ex)
            {
                //ekrandaGoster(MessageType.Error, "There  is  an  error  while
opening port. Check environment settings." + "\n");
                return false;
            }
        }
        #endregion

        #region PORT KAPA
        public bool portKapa()
        {
            try
            {
                if (serialPort1.IsOpen == false)
                {
                    ekrandaGoster(MessageType.Normal,    "Port    is    already
closed." + DateTime.Now + "\n");
                    return false;
                }
                else if (serialPort1.IsOpen == true)
                {
                    serialPort1.DataReceived -= serialPort_DataReceived;
                    serialPort1.DiscardInBuffer();
                    serialPort1.DiscardOutBuffer();
                    ekrandaGoster(MessageType.Normal,  "Port  is  closed."  +
DateTime.Now + "\n");
                    serialPort1.Close();
                    return true;
```

```
                }
                else return false;
            }
            catch (Exception ex)
            {
                ekrandaGoster(MessageType.Error,  "Error  while  closing  port.
Check environment settings." + "\n");
                return false;
            }
        }
        #endregion Port Kapama

        #region comPort_DataReceived

        /// <summary>
        /// method that will be called when theres data waiting in the buffer
        /// </summary>
        /// <param name="sender"></param>
        /// <param name="e"></param>
        delegate void SetTxt(string text);
        void              serialPort_DataReceived(object              sender,
SerialDataReceivedEventArgs e)
        {

            byte[] bufferRead = new byte[300];
            veriGeldi = true;
            try
            {
                if (serialPort1.BytesToRead > 0)
                {
                    byte[] bfr = new byte[serialPort1.BytesToRead];
                    serialPort1.Read(bfr, 0, bfr.Length);
                    UTF8Encoding enc = new UTF8Encoding();
                    string income = enc.GetString(bfr, 0, bfr.Length);
                    StrSet(income);
                }
            }
            catch (Exception ex)
            {
                //MessageBox.Show(ex.Message.ToString());
                return;
            }

        }

        public void StrSet(string s)
        {
            if (rtb1.InvokeRequired)
            {
                SetTxt tx = new SetTxt(StrSet);
                Invoke(tx, new object[] { s });
            }
            else
            {
                rtb1.Text = s.ToString();
            }
        }

        #endregion comPort_DataReceived

        #region DIGER
        private void SetRoleDurum(string role, string durum)
```

61

```csharp
        {
            string controlLed = role.Split('e')[1];
            int numVal = Convert.ToInt32(controlLed);
            if (role_durumlar[numVal - 1].Equals(durum))
            {
                ekrandaGoster(MessageType.Normal, "Role is already" + durum +
DateTime.Now + "\n");
            }
            else
            {
                role_durumlar[numVal - 1] = durum;
                ekrandaGoster(MessageType.Normal, "Role  is  " + durum +
DateTime.Now + "\n");
            }
        }

        private void btnRun_Click(object sender, EventArgs e)
        {
            string k = givenTime.Text;
            int sure = Convert.ToInt32(k);
            string btnName;
            string gidecek="";
            if (btnRun.Text.Equals("RUN"))
            {
                if (serialPort1.IsOpen == false)
                {
                    serialPort1.Open();
                    btnRun.Text = "STOP";
                    btnName = "role1";
                    gidecek = "[burayı protokole göre doldur]";//unutma
                    SetRoleDurum(btnName, "ON");
                    portAc(gidecek);

                    btnName = "role2";
                    gidecek = "[burayı protokole göre doldur]";//unutma
                    SetRoleDurum(btnName, "ON");
                    portAc(gidecek);

                    timer1.Enabled = true;
                    zaman = sure * 60;
                    dak = zaman / 60;
                    sn = zaman - (dak * 60);
                    if (sn == 60) sn = 00;
                    lblMin.Text = dak.ToString();
                    lblSec.Text = sn.ToString();
                }
                else ekrandaGoster(MessageType.Normal, "Already running\n");
            }
            else
            {
                if (serialPort1.IsOpen == true)
                {
                    portKapa();
                    btnRun.Text = "RUN";
                }
                else ekrandaGoster(MessageType.Normal, "Already stopped\n");
            }
        }

        private void timer1_Tick(object sender, EventArgs e)
        {
```

```csharp
            zaman--;
            dak = zaman / 60;
            lblMin.Text = dak.ToString();
            sn = zaman - (dak * 60);
            if (sn == 60) sn = 00;
            lblSec.Text = sn.ToString();
            if (zaman == 0)
            {
                string roleName;
                string gidecek = "";
                roleName = "role1";
                gidecek = "[burayı protokole göre doldur]";//unutma
                SetRoleDurum(roleName, "OFF");

                roleName = "role2";
                gidecek = "[burayı protokole göre doldur]";//unutma
                SetRoleDurum(roleName, "OFF");

                timer1.Enabled = false;
                btnRun.Text = "RUN";
            }
        }
        #endregion DIGER
    }
}
```

B. PREDOMINANCE DIAGRAM CALCULATIONS

Rxn 1 $\quad 2Ce + {}^3/_2 O_2 \leftrightarrow Ce_2O_3$

Rxn 2 $\quad Ce + O_2 \leftrightarrow CeO_2$

Rxn 3 $\quad Ce_2O_3 + {}^1/_2 O_2 \leftrightarrow 2CeO_2$
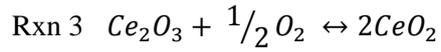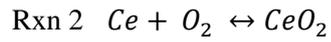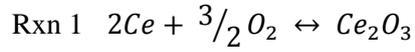
For Rxn 1 $\qquad \ln(K_{Rxn1}) = P_{O_2}{}^{-1.5}$

For Rxn 2 $\qquad ln(K_{Rxn2}) = P_{O_2}{}^{-1}$

For Rxn 2 $\qquad ln(K_{Rxn3}) = P_{O_2}{}^{-0.5}$

Table 10. ln(K) values for CeO_2 and Ce_2O_3

Temperature (K)	$ln(K)$	
	CeO2	Ce2O3
298.15	179.642	299.221
300	178.466	297.281
400	131.091	219.141
500	102.69	172.325
600	83.773	141.163
700	70.273	118.939
800	60.156	102.295
900	52.293	89.368
1000	46.006	79.039
1100	40.844	70.557
1200	36.53	63.466

$K_{Rxn1} = K_{Ce_2O_3}$

$K_{Rxn2} = K_{CeO_2}$

$K_{Rxn3} = 2K_{CeO_2} - K_{Ce_2O_3}$

Table 11. ln(K) values of reactions

Temperature (K)	$ln(K)$		
	1. rxn	**2. rxn**	**3. rxn**
298.15	179.642	299.221	60.063
300	178.466	297.281	59.651
400	131.091	219.141	43.041
500	102.69	172.325	33.055
600	83.773	141.163	26.383
700	70.273	118.939	21.607
800	60.156	102.295	18.017
900	52.293	89.368	15.218
1000	46.006	79.039	12.973
1100	40.844	70.557	11.131
1200	36.53	63.466	9.594

Table 12. $\ln(P_{O_2})$ values of reactions

Temperature (K)	$ln(P_{O_2})$		
	1. rxn	**2. rxn**	**3. rxn**
298.15	-199.481	-179.642	-120.126
300	-198.187	-178.466	-119.302
400	-146.094	-131.091	-86.082
500	-114.883	-102.69	-66.11
600	-94.1087	-83.773	-52.766
700	-79.2927	-70.273	-43.214
800	-68.1967	-60.156	-36.034
900	-59.5787	-52.293	-30.436
1000	-52.6927	-46.006	-25.946
1100	-47.038	-40.844	-22.262
1200	-42.3107	-36.53	-19.188

C. EQUILIBRIUM CONVERSION CALCULATIONS

$\Delta G_{rxn} = \left(\Delta G_{Ce_2O_3} + \frac{1}{2}\Delta G_{O_2}\right) - (2 * \Delta G_{CeO_2})$ at a specific temperature

$\Delta G_{rxn} = -RTln(K)$

$K = \exp(\dfrac{-1 * \Delta G_{rxn}}{R * T})$

Where $R = 0.008314 \, ^{kJ}/_{mol.K}$

$X_e = K/(1 + K)$

Table 13. Gibbs energy of formation table of CeO_2, Ce_2O_3 and O_2

Temperature (K)	ΔGf (kJ/mol)		
	CeO2	Ce2O3	O2
298.15	-1025.38	-1707.93	0
300	-1024.99	-1707.38	0
400	-1003.87	-1678.13	0
500	-982.968	-1649.53	0
600	-962.268	-1621.48	0
700	-941.729	-1593.9	0
800	-921.316	-1566.7	0
900	-901.002	-1539.8	0
1000	-880.76	-1513.16	0
1100	-860.135	-1485.84	0
1200	-839.207	-1458.01	0
1300	-818.279	-1430.18	0
1400	-797.351	-1402.35	0
1500	-776.423	-1374.52	0
1600	-755.495	-1346.69	0
1700	-734.567	-1318.86	0
1800	-713.639	-1291.03	0
1900	-692.711	-1263.19	0
2000	-671.783	-1235.36	0
2100	-650.855	-1207.53	0
2200	-629.927	-1179.7	0
2300	-608.999	-1151.87	0
2400	-588.071	-1124.04	0
2500	-567.143	-1096.21	0

Table 14. Gibbs energy of reaction results, K results and equilibrium conversion results for O_2 desorption from pure CeO_2 reaction

Temperature	ΔGrxn (kJ/mol)	K	Xe
298.15	342.833	8.60825E-61	8.61E-61
300	342.597	2.22029E-60	2.22E-60
400	329.607	9.04041E-44	9.04E-44
500	316.411	8.78166E-34	8.78E-34
600	303.052	4.13073E-27	4.13E-27
700	289.555	2.46809E-22	2.47E-22
800	275.933	9.6111E-19	9.61E-19
900	262.201	6.04924E-16	6.05E-16
1000	248.363	1.06262E-13	1.06E-13
1100	234.428	7.37125E-12	7.37E-12
1200	220.403	2.54543E-10	2.55E-10
1300	206.378	5.09719E-09	5.1E-09
1400	192.353	6.65216E-08	6.65E-08
1500	178.328	6.16372E-07	6.16E-07
1600	164.303	4.32378E-06	4.32E-06
1700	150.278	2.41186E-05	2.41E-05
1800	136.253	0.000111147	0.000111
1900	122.228	0.000436111	0.000436
2000	108.203	0.001492539	0.00149
2100	94.178	0.004543242	0.004523
2200	80.153	0.012498478	0.012344
2300	66.128	0.031487032	0.030526
2400	52.103	0.073445767	0.068421
2500	38.078	0.160093986	0.138001

D. METAL DISPERSION CALCULATIONS

Table 15. Stoichiometric factors for some metals

Metal (M)	H_2/M	CO/M	O_2/M
Pt	0.5	1 – 1.15	0.5
Pd	0.5	0.6	-
Os	0.5	-	-
Ni	0.5	-	-
Co	0.5	-	-
Fe	0.5	0.5	-
Ag	-	-	0.4
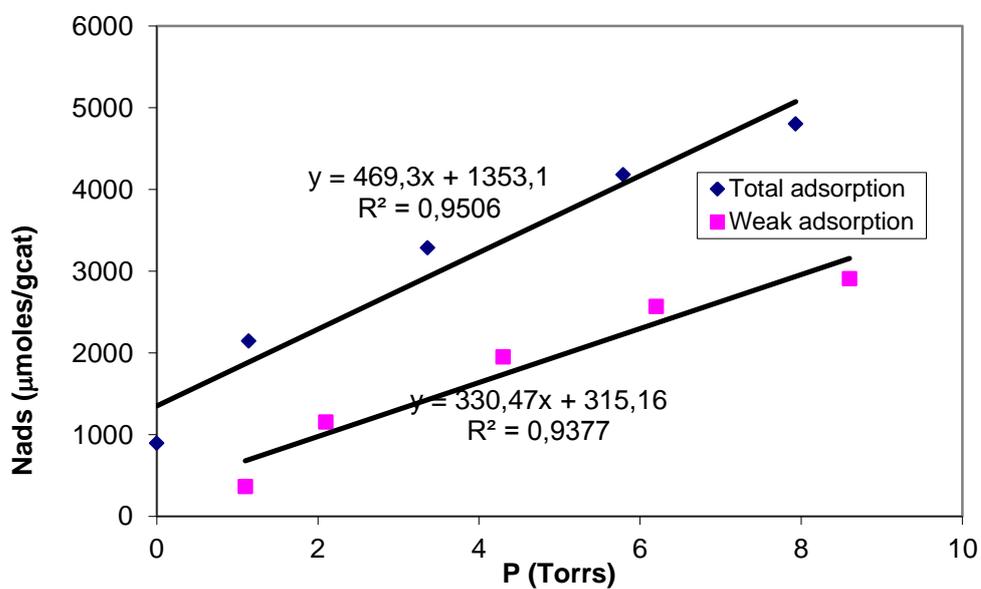
Figure 47. Adsorption points for reflux catalyst
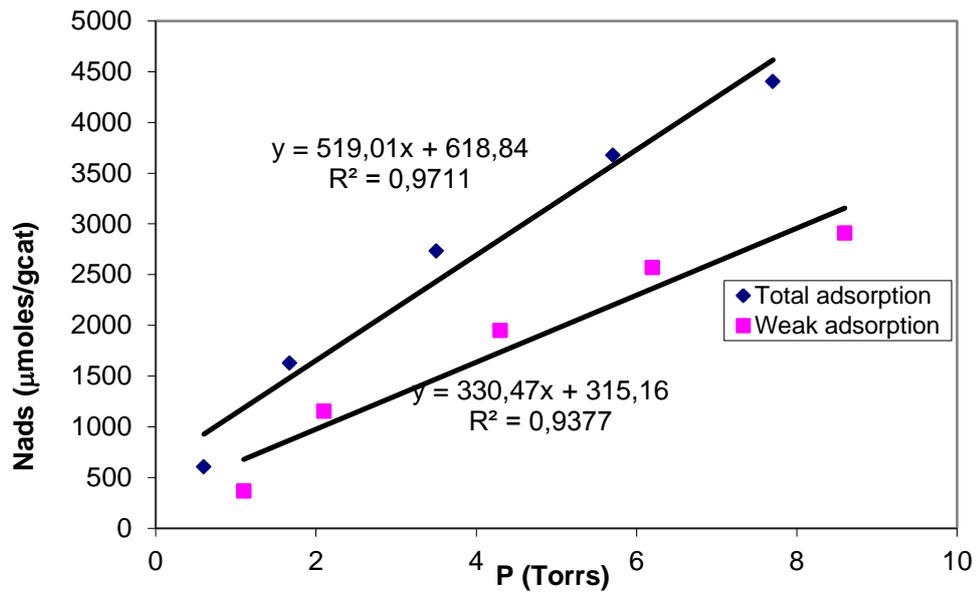
Figure 48. Adsorption points for incipient wetness catalyst

$$MD = \frac{(V_m \; x \; A_W \; x \; 10^4)}{(W \; x \; S_f)}$$

Where;

MD = metal dispersion percentage

V_m = monolayer volume (moles of gas per gram of sample)

A_W = metal atomic weight (gram of metal per mole)

W = metal percentage in the sample

S_f = stoichiometric factor (molecule of gas per metal atom)

H_2 is used for dispersion experiments.

S_f = 0.5 for H_2/Pt from table 13.

A_W = 195 g/mole for Pt

W = 1 %

V_m = 1353.1 moles H_2 / gcat for reflux catalyst from figure 47

V_m = 618.84 moles H_2 / gcat for incipient wetness catalyst from figure 48

For reflux catalyst;

MD = 52.9 %

69

For incipient wetness catalyst;

MD = 24.2 %

E. OXYGEN SIGNAL CALIBRATION

Table 16. Oxygen volume vs integrated area table for calibration

oxygen volume (uL)	Area
100	4.52748E-07
250	1.13756E-06
500	2.93838E-06
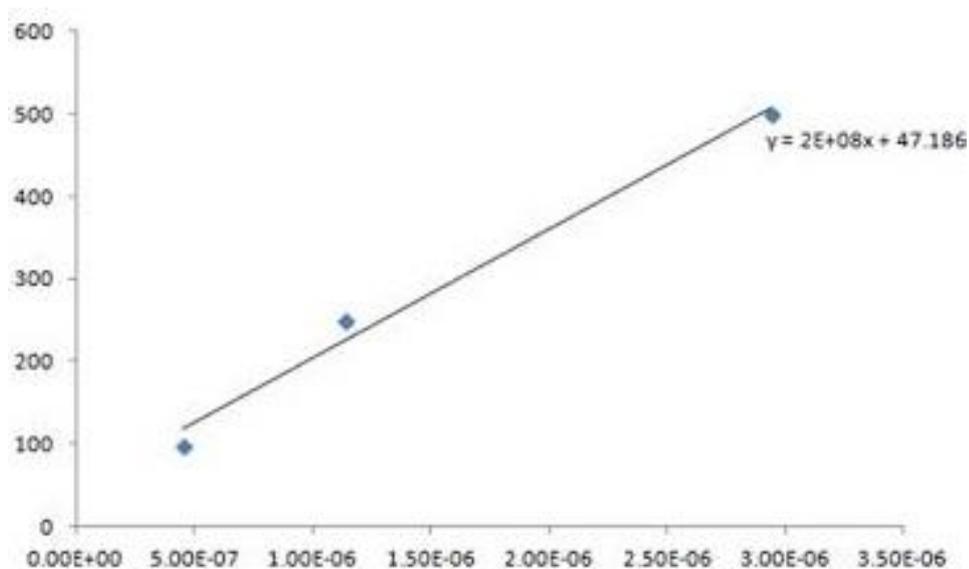
Figure 49. Adsorption points for incipient wetness catalyst

Calibration equation from data at table 18 is $y = (2x10^8)x + 47.186$. Table 19 shows the results of oxygen TPD experiments. Oxygen desorption volume amounts are calculated by putting integrated area instead of x in calibration equation.

Table 17. Integrated area vs desorbed oxygen amount table

Catalyst	Integrated Area	Oxygen Desorption Amount (uL)
Reflux	1.12361E-06	224.72
First Cycle	6.73507E-07	134.70
Second Cycle	1.9158E-07	38.32
Third Cycle	1.983E-07	39.66
Fourth Cycle	2.18921E-07	43.78
Fifth Cycle	1.84118E-07	36.82

F. EXPERIMENT PROCEDURES

F1. CO_2 Desorption Experiments

1. CO_2 desorption experiments were conducted in TPD system with MS set-up described in section 3.3.2. Before starting the experiment 100 mg catalyst was carefully weighed and placed in a quartz reactor which has 6 mm diameter. 30 sccm nitrogen was fed to the reactor while temperature was increased up to 900^0C with 5^0C / min heating rate to be desorbed all adsorbed H_2O, CO_2 and O_2 molecules.
2. After is the temperature reached to 900^0C, it is cooled again to room temperature (30 sccm nitrogen effluent is still continued)
3. 20 sccm CO_2 is given to the reactor for 30 minutes at room temperature.
4. After 30 minutes CO_2 effluent, nitrogen gas is given to the reactor again.
5. One should continue to give nitrogen gas to the system at room temperature until CO_2 signal of MS becomes stable.
6. After the signal is become stable, temperature is started to rise to 400^0C with 20^0C / min heating rate.
7. While the temperature is rising to 400^0C, CO_2 signal of MS is collected by PC.

F2. H_2O Desorption Experiments

1. 100 mg catalyst is put into reactor.
2. 30 sccm nitrogen is given to the reactor while temperature is increasing up to 900^0C with 5^0C / min heating rate.
3. After reactor is reached to 900^0C, it is cooled again to room temperature (30 sccm nitrogen effluent is still continued)
4. 20 sccm air with moisture is given to the reactor for 30 minutes at room temperature. To give moisture, air goes through some water before enter the reactor.
5. After 30 minutes air effluent, nitrogen gas is given to the reactor again.
6. One should continue to give nitrogen gas to the system at room temperature until H_2O signal of MS becomes stable.
7. After the signal is become stable, temperature is started to rise to 400^0C with 20^0C / min heating rate.
8. While the temperature is rising to 400^0C, H_2O signal of MS is collected by PC.

F3. O_2 Desorption Experiments

1. 100 mg catalyst is put into reactor.

2. 30 sccm nitrogen is given to the reactor while temperature is increasing up to 1300^0C with 5^0C / min heating rate.
3. After reactor is reached to 1300^0C, it is cooled again to room temperature (30 sccm nitrogen effluent is still continued)
4. 20 sccm O_2 is given to the reactor for 30 minutes at room temperature.
5. After 30 minutes air effluent, nitrogen gas is given to the reactor again.
6. One should continue to give nitrogen gas to the system at room temperature until O_2 signal of MS becomes stable.
7. After the signal is become stable, temperature is started to rise to 1300^0C with 20^0C / min heating rate.
8. While the temperature is rising to 1300^0C, O_2 signal of MS is collected by PC.

F4. Dispersion Experiments

F4.1   Method of gas injection into the system

1. First, all the system is taken in vacuum.
2. Pressure of gas is arranged to slightly above than atmospheric pressure from the regulator of gas tube.
3. VFP1 valve is turned to the direction of H2 gas.
4. VTP1 valve is turned to S1 direction.
5. VV3 and VV4 valves are closed and VV5 valve is opened.
6. Pressure data is recorded as 0.
7. After VV1 valve is slightly opened, VN1 valve is also slightly opened.
8. It is seen that pressure data is started to rise.
9. After 1 minute, VV4 and VV6 valves are opened.
10. After 1 minute, VV5 valve is closed.
11. Waiting until pressure is stabilizing.
12. VV1, VN1, VV4 and VV6 valves are closed respectively.

F4.2   Dispersion experiment procedure

1.   Sample is weighted and put into sample holder.
2.   Furnace is adjusted to the position of heating sample holder.
3.   Dead volume of the system is measured.
4.   Reduction of sample is done.
5.   Total adsorption and weak adsorption measurements are done.

F4.3   Dead volume measurement

1. An inert gas is given to the system by method of gas injection into the system.
2. After the gas is given into system, VV5 valve is opened.
3. After pressure is stabilized, VV5 valve is closed.
4. Pressure data is taken as P1.
5. VV3 valve is opened .

6. After 5 minutes, pressure data is taken as P2.
7. VV3 valve is closed and pressure data is taken as P3.
8. Dead volume is calculated by P1V1=P2V2 principle.

F4.4   Reduction Procedure

1. System is taken into vacuum.
2. H2 gas is taken into system by method of gas injection into the system.
3. After H2 gas is given into system, pressure of system is adjusted to 100 Torr by opening VV5 valve.
4. VV3 valve is opened.
5. Furnace temperature is set to 3500C.
6. After the furnace temperature is become 3500C, one should be waited for half an hour.
7. VV3 and VV5 valves are opened while VV4 and VV6 valves in closed position. Manifold and sample holder are vacuumed for 5 minutes.
8. VV5 valve is closed.
9. VV4 and VV6 valves are opened and H2 gas is given into the system again.
10. Pressure should be 500 Torr.
11. VV4, VV5 and VV6 valves are closed while VV3 valve in open position. One should be waited for 30 minutes.
12. Step 7,8,9,10 and 11 are done 2 more times.
13. Close the furnace and wait for 2 hours while VV3, VV4, VV5 and VV6 in open position.

F4.5   Dispersion Procedure

Total Adsorption:

1. H2 gas is taken into system by method of gas injection into the system.
2. H2 pressure in manifold is adjusted to 2 Torr by opening VV5 valve.
3. After pressure is become about 2 Torr, VV5 valve is closed.
4. This pressure data is taken P1.
5. VV3 valve is opened. After 5 minutes, pressure data is taken as P2.
6. VV3 is closed and pressure data is taken as P3.
7. Pressure is adjusted to the needed value by using VV4 and VV6 valves. (4 Torr, 6 Torr, 8 Torr and 10 Torr for different points)
8. After VV4 and VV6 are closed, pressure data is taken as P1.
9. VV3 valve is opened. After 5 minutes, pressure data is taken as P2.
10. VV3 is closed and pressure data is taken as P3.
11. Step 7,8,9 and 10 are done 3 more times.
12. Finally, sample holder and manifold are vacuumed while VV4 and VV6 valves in close position and VV3 and VV5 in open position.

Weak Adsorption:

1. After sample holder and manifold are vacuumed, H2 gas is taken into system by method of gas injection into the system.
2. H2 pressure in manifold is adjusted to 2 Torr by opening VV5 valve.
3. After pressure is become about 2 Torr, VV5 valve is closed.
4. This pressure data is taken P1.
5. VV3 valve is opened. After 5 minutes, pressure data is taken as P2.
6. VV3 is closed and pressure data is taken as P3.
7. Pressure is adjusted to the needed value by using VV4 and VV6 valves. (4 Torr, 6 Torr, 8 Torr and 10 Torr for different points)
8. After VV4 and VV6 are closed, pressure data is taken as P1.
9. VV3 valve is opened. After 5 minutes, pressure data is taken as P2.
10. VV3 is closed and pressure data is taken as P3.
11. Step 7,8,9 and 10 are done 3 more times.
12. Finally, sample holder and manifold are vacuumed while VV4 and VV6 valves in close position and VV3 and VV5 in open position.